Organic & Biomolecular Chemistry

ROYAL SOCIETY OF CHEMISTRY

PAPER

View Article Online
View Journal





Cite this: DOI: 10.1039/d0ob00078g

# A modular approach to the bisbenzylisoquinoline alkaloids tetrandrine and isotetrandrine†‡

Ramona Schütz, [a] Maximilian Meixner,[b] Iris Antes*[b] and Franz Bracher *[a]

Received 14th January 2020,
Accepted 13th February 2020

DOI: 10.1039/d0ob00078g

rsc.li/obc

An efficient racemic total synthesis of the bisbenzylisoquinoline alkaloids tetrandrine and isotetrandrine in four different routes is reported herein. Key steps of the synthesis include *N*-acyl Pictet–Spengler condensations to access the tetrahydroisoquinoline moieties, as well as copper-catalyzed Ullmann couplings for diaryl ether formation. Starting from commercially available building blocks tetrandrine and isotetrandrine are accessed in 12 steps. Depending on the sequence of the four central condensation steps, equimolar mixtures of both diastereomers or predominantly tetrandrine or its diastereomer isotetrandrine are obtained. Through computational analysis we were able to rationalize the differences in the observed diastereomeric specificities.

## Introduction

Tetrandrine (**1**) is a bisbenzylisoquinoline alkaloid isolated from *Stephania tetrandra* (Menispermaceae), a climbing plant native to Asia.[1] This herb has been used in Chinese and Japanese traditional medicine for treating a variety of diseases such as tuberculosis, malaria, asthma, hyperglycaemia, hypertension and cancer.[2] First isolated in 1928 by Kondo and Yano,[3,4] tetrandrine (**1**) was identified as one of the active agents of the herb. Far beyond the traditional use the pharmacological effects of tetrandrine (**1**) in its pure form have been subject of numerous studies. Most importantly, tetrandrine (**1**) has been identified as an antagonist of calcium channels.[5,6] Thereby two-pore channels (TPC), voltage gated calcium channels located on lysosomal membranes,[7] emerged as an interesting pharmacological target recently, since they play a role in the pathomechanism of diseases such as Ebola virus infection and cancer.[8–10] Hereby, tetrandrine (**1**) was shown to be a potent inhibitor of Ebola virus entry *in vivo* as well as *in vitro* in sub-micromolar concentrations ($IC_{50}$ value of 55 nM) through inhibiting TPC channels (Fig. 1).[8]

TPC channels are also involved in tumor metastasis.[9] Nguyen *et al.*[9] demonstrated that cancer cell migration can be reduced by pharmacological inhibition of TPC1 and TPC2 *in vitro* and *in vivo* using tetrandrine (**1**). Another important pharmacological target of tetrandrine (**1**) is P-glycoprotein (P-gp), a universal efflux pump for xenobiotics responsible for multidrug resistance of tumors. Overexpression of P-gp in cancer cells is a key factor of drug resistance towards a variety of structurally different antitumor agents.[12] Among a series of isoquinoline-type alkaloids, tetrandrine (**1**) was identified as an outstanding inhibitor of P-gp.[13,14] Under the name CBT-1™ this alkaloid has advanced to clinical studies.[15]

Previous efforts in antitumor drug discovery evolved a number of semi-synthetic tetrandrine derivatives. Hereby, structural modifications started from this compound, available from plant sources and mainly focused on introduction of substituents on C-5[16–18] as well as C-14[19–21] by electrophilic substitution reactions on the electron-rich aromatic rings, further on *N*-alkylation at N-2′ to give quaternary ammonium salts.[22]

Besides its heterogeneous pharmacological profile also possible toxic side effects were reported for tetrandrine (**1**).[23]

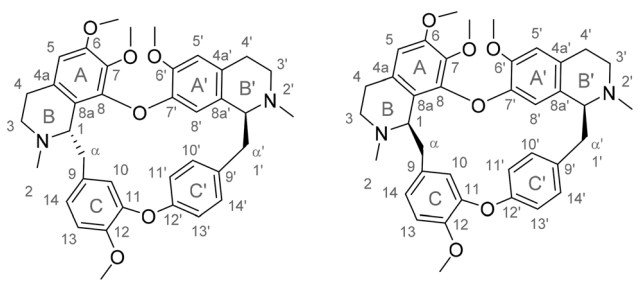

**Fig. 1** Tetrandrine (**1**) (1S,1′S) and isotetrandrine (**2**) (1R,1′S) – Numbering of the skeleton according to the convention established by Shamma.[11]

[a]*Department of Pharmacy – Center for Drug Research, Ludwig-Maximilians University Munich, Butenandtstr. 5-13, 81377 Munich, Germany. E-mail: Franz.Bracher@cup.uni-muenchen.de*

[b]*TUM School of Life Sciences, Technical University Munich, Emil-Erlenmeyer-Forum 8, 85354 Freising, Germany*

†In memory of Prof. Dr Peter Pachaly, a pioneer in the field of bisbenzylisoquinoline alkaloids, who passed away on January 10, 2019.

‡Electronic supplementary information (ESI) available. See DOI: 10.1039/d0ob00078g

Oxidative metabolism involving the methoxy group at C-12 results in the formation of a highly reactive quinone methide prone to reaction with bio-nucleophiles, and suspected to be responsible for pulmonary damage in animal models.[24,25] Furthermore, after continuous administration of tetrandrine (**1**) a pathological change of liver tissues was observed in dogs.[26]

All of these data make tetrandrine (**1**) a very interesting lead compound for further development as a chemical tool for pharmacological studies and as a drug candidate. Systematic structure modifications should pave the way for increasing selectivity and decreasing toxicity. Since options for semi-synthetic variations starting from tetrandrine (**1**) from plant sources are limited and likely to be already exploited we aimed to develop a new synthetic route allowing to flexibly implement diverse structure variations.

The first published total synthesis of tetrandrine (**1**), its enantiomer phaeanthine, and its diastereomer isotetrandrine (**2**) by Inubushi and coworkers, first published in 1968,[27,28] implies more than 20 steps. Key steps are two copper-mediated Ullmann couplings for the formation of the diaryl ether moieties and two Bischler–Napieralski reactions for the construction of the two benzylisoquinoline units. The final steps of this total synthesis are an intramolecular Bischler–Napieralski cyclization, followed by reduction of the resulting dihydroisoquinoline intermediate and *N*-methylation. Very recently, a similar approach using the same key reactions was published in a Chinese patent.[29] This approach includes two successive Ullmann couplings of racemic benzyltetrahydroisoquinoline units as the final steps, and consequently lacks stereoselectivity.

Hereafter, we present a new 12 step total synthesis of racemic tetrandrine (*rac*-**1**) and its diastereomer isotetrandrine (*rac*-**2**).

## Results and discussion

In contrast to the published total syntheses of tetrandrine (**1**), our retrosynthetic approach aimed at utilizing *N*-acyl Pictet–Spengler cyclizations instead of Bischler–Napieralski protocols. This approach would provide *tetra*hydroisoquinolines directly, and further, by using *N*-alkoxycarbonyl residues in the *N*-acylarylethylamine building blocks, the required *N*-methyl groups should be available in only one additional step by lithium alanate reduction of the carbamate groups. This should lead to a significant reduction of the required number of steps. Alternatively, hydrolysis of the carbamate groups would provide secondary amino groups (*N*-2-*H*, *N*-2′-*H*), which in turn could subsequently be *N*-alkylated to give various tertiary amino groups. Further, ώ-alkoxystyrenes (instead of unstable arylacetaldehydes) were envisaged as building blocks for the *N*-acyl Pictet–Spengler cyclizations following Comins' approach.[30] This should reduce the number of steps further compared to the original method, since ώ-alkoxystyrenes are available from the corresponding substituted benzaldehydes in one single step, whereas construction of arylacetic acids for Bischler–Napieralski reactions requires a number of steps. Further, we aimed at exploring modern alternatives such as Buchwald–Hartwig coupling[31] or Chan–Evans–Lam reaction[32] for the construction of the diaryl ether moieties.

Based on these considerations several alternative routes to tetrandrine (**1**) (and its isomers) were explored: In route 1 both 1-benzyltetrahydroisoquinoline moieties – meaning both stereocenters at C-1 and C-1′ in consequence – were to be built up early in *inter*molecular *N*-acyl Pictet–Spengler reactions, and the central step for the construction of the macrocycle should be an *intra*molecular diaryl ether synthesis at a late stage. In contrast, in route 2 a late *intra*molecular *N*-acyl Pictet–Spengler cyclization should provide the macrocycle under construction of the second stereocenter. For each route an additional variation was designed, considering that either the benzyltetrahydroisoquinoline moiety consisting of rings A–C or the one consisting of rings A′–C′ can be constructed first. Besides the general feasibility of both approaches, the stereochemical outcome of all four conceivable variants was of high interest, as high diastereoselectivity of the whole protocol was desirable.

The sequence of the Pictet–Spengler- and Ullmann-type steps of the four variants is depicted in Fig. 2. In detail, in the variants 1a and 1b the retrosynthetic approach for the syn-

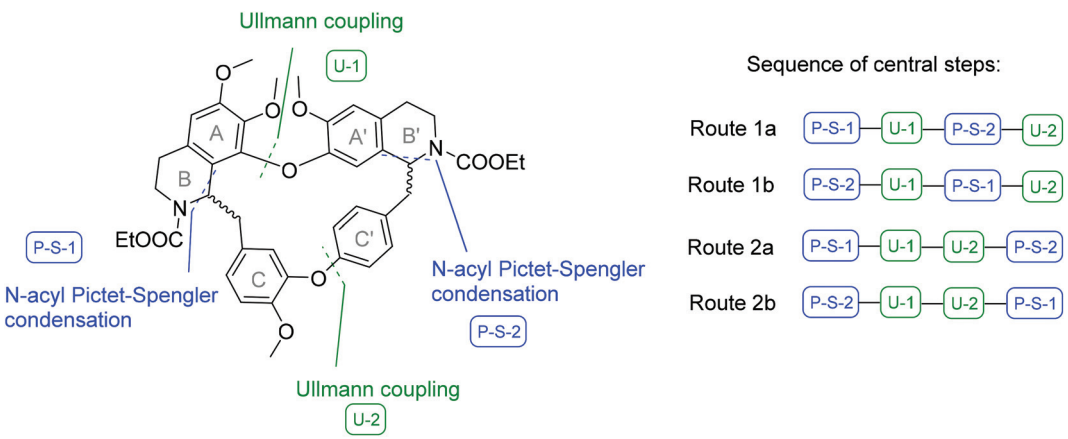


**Fig. 2** Retrosynthetic analysis of the envisaged routes to tetrandrine precursor **15**.

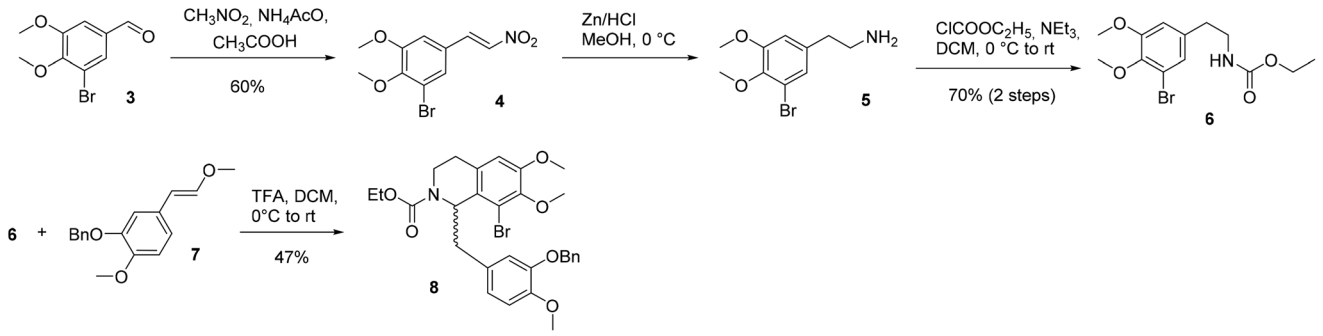


Scheme 1 Route 1a: Synthesis of the benzyltetrahydroisoquinoline **8**.

thesis of the macrocyclic skeleton consists of two alternating *N*-acyl Pictet–Spengler condensations and C–O couplings. Finally the macrocycle is generated in an *intra*molecular Ullmann coupling ("U-2") of a seco-bisbenzylisoquinoline intermediate, connecting rings C and C′. In route 2, both diaryl ethers are constructed early (operations "U-1" and "U-2"), and the macrocycle is generated in an *intra*molecular *N*-acyl Pictet–Spengler condensation, whereby in route 2a ring B′ is constructed in this late operation ("P-S-2"), whereas in route 2b this final connection is performed for construction of ring B ("P-S-1").

In route 1a the highly substituted 1-benzyltetrahydroisoquinoline **8**, which covers rings A–C of tetrandrine (**1**), was prepared from the commercially available aldehydes 5-bromoveratraldehyde (**3**) and *O*-benzylisovanilline. In a Henry reaction **3** was condensed with nitromethane[33] to give β-nitrostyrene **4** in 60% yield. Reduction with zinc/HCl[33] gave the corresponding arylethylamine **5**, and subsequent reaction with ethyl chloroformate led to carbamate **6** in 70% yield over both steps. Known enol ether **7**[34] was synthesized in a Wittig olefination of *O*-benzylisovanilline in 87% yield. The following *N*-acyl Pictet–Spengler condensation[30] with carbamate **6**, catalyzed by trifluoroacetic acid (TFA), gave racemic tetrahydroisoquinoline **8** in 47% yield (Scheme 1). This moderate yield might be due to the sterically demanding bromine substituent. We tried to enhance the yield by using trifluoromethanesulfonic acid (TfOH) as a stronger acidic catalyst[35] and obtained **8** in a comparable yield of 49%. But due to easier handling we preferred using TFA in the following procedures. The *N*-acyl Pictet–Spengler condensation in this step delivers exclusively the desired regioisomer **8**. There was no by-product found in which cyclization took place at the *para* position of bromine.

Next, the first C–O coupling was performed in order to obtain diaryl ether **11** (Scheme 2). The required phenol **10** was prepared from commercially available 3-methoxytyramine (**9**; itself readily available from the aromatic aldehyde vanilline) and ethyl chloroformate. For the coupling of **8** with **10** several reaction conditions (Table 1) were explored testing different ligand/catalyst systems. Palladium-catalyzed Buchwald–Hartwig cross-coupling reactions (Table 1, entries 1–3) using different phosphine ligands[36] or Pd-PEPPSI™-IPr as catalyst failed to furnish the desired diaryl ether **11**. Next a set of catalytic systems for Ullmann-type C–O couplings was explored employing different combinations of copper(I) halides, ligands and bases (entries 4–8). Using the combination of copper(I) iodide, *N*,*N*-dimethylglycine and caesium carbonate in dioxane[37] we were able to detect traces of the desired product **11** (entry 4) by LC-MS. Increasing catalyst and ligand to stoichiometric amounts did not improve the yields. Employing copper(I) bromide-dimethylsulfide complex with caesium carbonate in pyridine[38] without any additional ligand (entry 9) we were able to isolate minor amounts (2%) of the desired diaryl

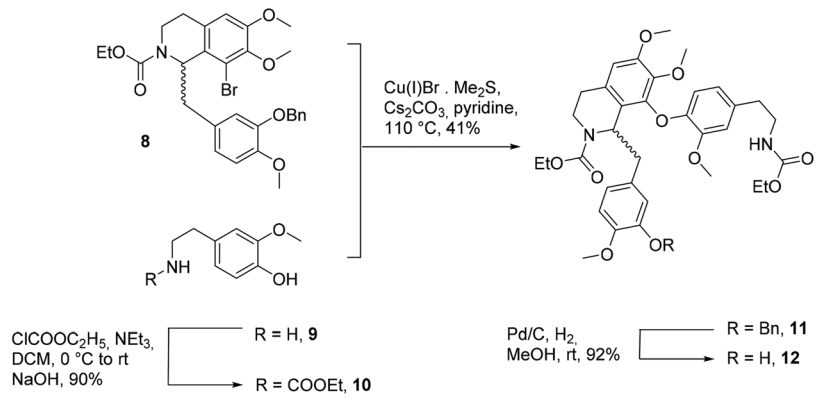


Scheme 2 Route 1a: First Ullmann coupling.

**Table 1** Conditions for Ullmann-type C–O coupling

| Entry | Conditions | Equiv. phenol **10** | Yield (%) |
|---|---|---|---|
| 1 | $Pd_2(dba)_3$ (1.5 mol%), *t*BuXPhos (2.0 mol%), $K_3PO_4$ (2.0 equiv.), toluene, 100 °C, 48 h (ref. 36) | 1.2 | — |
| 2 | $Pd(AcO)_2$ (5.0 mol%), $Me_4$*t*ButylXphos (7.0 mol%), $K_3PO_4$ (2.0 equiv.), toluene, 100 °C, 48 h (ref. 36) | 1.2 | — |
| 3 | PEPPSI-IPr (2.0 mol%), $K_3PO_4$ (2.0 equiv.), toluene, 100 °C, 48 h | 1.2 | — |
| 4 | CuI (0.1 equiv.), *N*,*N*-dimethylglycine (0.3 equiv.), $Cs_2CO_3$ (2.0 equiv.), dioxane, 105 °C, 72 h, pressure tube (ref. 37) | 1.5 | Traces |
| 5 | CuI (1.0 equiv.), *N*,*N*-dimethylglycine (3.0 equiv.), $Cs_2CO_3$ (2.0 equiv.), dioxane, 105 °C, 72 h, pressure tube (ref. 37) | 1.5 | Traces |
| 6 | CuI (0.1 equiv.), *N*,*N*-dimethylglycine (0.3 equiv.), $Cs_2CO_3$ (2.0 equiv.), dioxane, 150–200 °C, 2.5 h, microwaves (ref. 39) | 1.5 | — |
| 7 | CuI (0.1 equiv.), picolinic acid (0.2 equiv.), $K_3PO_4$ (2.0 equiv.), DMSO, 90 °C, 72 h (ref. 41) | 1.2 | — |
| 8 | CuBr (1.0 equiv.), 1,1′-azo*bis*(cyclohexane carbonitrile) (1.0 equiv.), $Cs_2CO_3$ (2.0 equiv.), DMF, 100 °C, 4 h, microwaves (ref. 42) | 1.1 | — |
| 9 | CuBr·$Me_2S$ (1.0 equiv.), $Cs_2CO_3$ (3.0 equiv.), pyridine, 150–200 °C, 72 h, pressure tube (ref. 38) | 1.1 | 2 |
| 10 | CuBr·$Me_2S$ (1.0 equiv.), $Cs_2CO_3$ (3.0 equiv.), pyridine, 220 °C, 3 h, microwaves | 1.1 | — |
| 11 | CuBr·$Me_2S$ (1.0 equiv.), $Cs_2CO_3$ (3.0 equiv.), pyridine, 110 °C, 7 d | 1.1 | 12 |
| 12 | CuBr·$Me_2S$ (1.0 equiv.), $Cs_2CO_3$ (3.0 equiv.), pyridine, 110 °C, 7 d | 1.5 | 27 |
| 13 | CuBr·$Me_2S$ (1.0 equiv.), $Cs_2CO_3$ (3.0 equiv.), pyridine, 110 °C, 7 d | 2.0 | 41 |

ether **11**. A predominant side reaction was debromination of the aryl halide **8** at high reaction temperatures. Microwave conditions[39,40] instead of conventional heating could not improve the reaction in terms of yield and by-product formation (entry 10). To minimize debromination we decreased the temperature to 110 °C and prolonged the reaction time. This modification resulted in a better yield (12%; entry 11). By increasing the amount of phenol **10** from 1.1 to 1.5 equivalents we were able to further improve the yield to 27% (entry 12). The best result was obtained when performing the reaction at 110 °C with 2.0 equivalents of the phenol **10** furnishing diaryl ether **11** in 41% yield (entry 13). Considering the comparatively low reactivity of electron-rich and sterically hindered aryl halide **8**, the obtained yield is satisfying and comparable to the yield of 42% in Inubushi's approach[27] using related building blocks. An attempted Chan–Lam–Evans coupling[32] was discarded after the synthesis of the corresponding boronic acid from bromoarene **8** was unsuccessful. Diaryl ether **11** was then *O*-debenzylated by standard Pd-catalyzed hydrogenolysis giving phenol **12** in 92% yield. The debenzylation had to be performed at this stage, since surprisingly the *O*-benzylated intermediate **11** was found to react very sluggishly in an attempted subsequent *N*-acyl Pictet–Spengler reaction with enol ether **13**.

For the construction of the second tetrahydroisoquinoline moiety our method of choice was again a TFA-mediated *N*-acyl Pictet–Spengler condensation, connecting intermediate **12** with known enol ether **13**[43] to give seco-bisbenzylisoquinoline **14** in an excellent yield of 96% (Scheme 3) and again with desired regioselectivity. As expected we obtained both racemic diastereomers in a ratio of 1 : 1 (determined by HPLC). No stereocontrol was observed, since the newly formed stereocenter is far away from the stereocenter in the starting material. But fortunately, the obtained diastereomers of **14** were easily

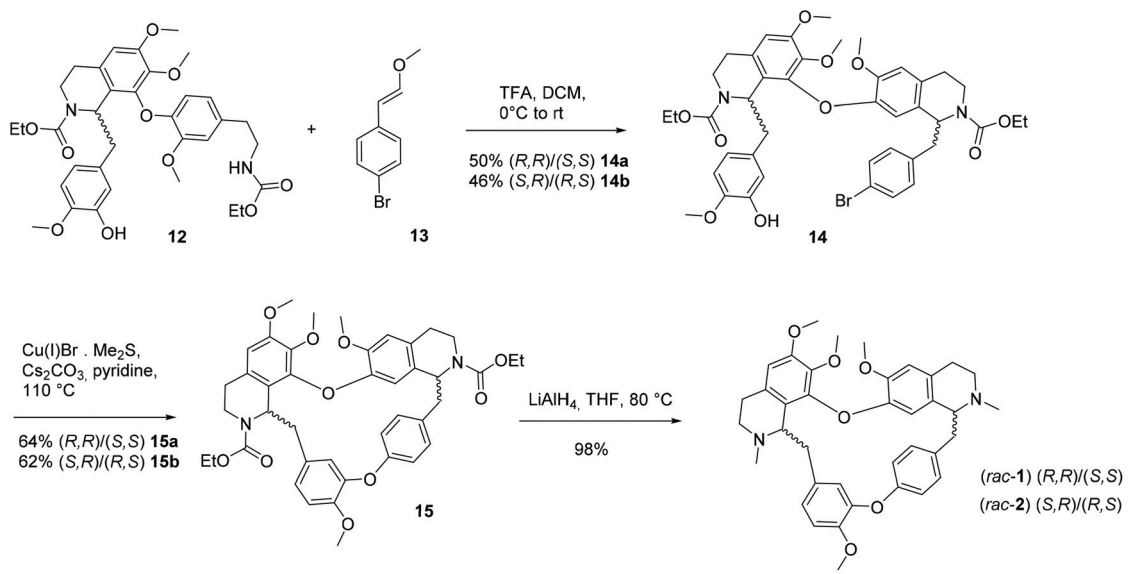


**Scheme 3** Route 1a: Synthesis of racemic tetrandrine (*rac*-1) and racemic isotetrandrine (*rac*-2) *via* seco-bisbenzylisoquinoline **14**.

 

separated by flash column chromatography on a preparative scale. The isolated yields of the racemic diastereomers were 50% of the (*R*,*R*)/(*S*,*S*) isomers (**14a**) and 46% of the (*R*,*S*)/(*S*,*R*) isomers (**14b**). The relative configurations of these products were determined retrospectively after conversion into racemic tetrandrine (*rac*-**1**) and racemic isotetrandrine (*rac*-**2**), respectively.

For the following intramolecular C–O coupling to generate the macrocycle **15** we once again conducted a screening for reaction conditions. $Pd_2(dba)_3$ in combination with phosphine ligand $Me_4$*t*ButylXphos,[36] copper(I) iodide combined with ligand *N*,*N*-dimethylglycine[37] and copper(I) bromide-dimethylsulfide complex[38] were tested as catalytic systems on a mixture of diastereomers **14** (compare entries 2, 4 and 11 in Table 1). All of these reactions were carried out under high dilution conditions (0.02 M) in order to suppress intermolecular coupling reactions. Again copper(I) bromide-dimethylsulfide complex catalyzed the diaryl ether synthesis well, furnishing the desired macrocycle **15** in 62–64% yield (Scheme 3), whereas the other catalytic systems failed. To our surprise, separation of diastereomers of **15** *via* flash column chromatography could not be achieved. Thus, for generation of pure racemic alkaloids the cyclization had to be conducted with the previously isolated racemic diastereomers of the seco-intermediate **14**. Both isomers were cyclized in almost identical yields of 62 and 64%.

To complete the total synthesis of the alkaloids, carbamates **15** were reduced using $LiAlH_4$ in THF to give racemic tetrandrine (*rac*-**1**) and racemic isotetrandrine (*rac*-**2**), both in almost quantitative yield (98%) (Scheme 3). The analytical data of racemic tetrandrine (*rac*-**1**) was identical with those of an authentic natural sample of tetrandrine (**1**), kindly donated by Prof. P. Pachaly.

As a variation of this approach we elaborated route 1b, which starts with the synthesis of the benzyltetrahydroisoquinoline unit consisting of rings A′–C′. Following the established protocol of TFA-catalyzed *N*-acyl Pictet–Spengler reaction, carbamate **10** was condensed with known enol ether **16**[44] to give racemic 1-benzyltetrahydroisoquinoline **17** in 96% yield (Scheme 4). Enol ether **16** was synthesized by Wittig olefination of commercially available 4-benzyloxybenzaldehyde in 97% yield. For the Ullmann synthesis of diaryl ether **18** from phenolic intermediate **17** and aryl bromide **6** (see Scheme 1) we once again employed the established catalytic system (Scheme 4).

This critical key step could significantly be enhanced in this approach compared to route 1a (Scheme 2). The diaryl ether was now obtained in a yield of 64% (*vs.* 41%) in a shorter reaction time (3 days *vs.* 7 days). Also in terms of efficiency this step was improved, since only 1.0 equiv. of phenol instead of 2.0 equiv. was brought to reaction with 1.2 equiv. of aryl bromide **6**. The improved yield can be explained by the fact that aryl bromide **6** is less sterically hindered than the aryl halide **8** in route 1a. Diaryl ether **18** was further debenzylated by hydrogenolysis in methanol to give phenol **19** in 94% yield (Scheme 4).

Next seco-bisbenzylisoquinoline **21** was obtained in an *N*-acyl Pictet–Spengler reaction of **19** with enol ether **20**,[45] which was prepared in 80% yield by Wittig olefination of the corresponding aromatic aldehyde. To our surprise (compared to route 1a) the product of this Pictet–Spengler reaction following our standard protocol was not an equimolar racemic mixture of diastereomers, but the (*R*,*R*)/(*S*,*S*) isomers (**21a**) were formed preferably (ratio 62 : 38, determined by HPLC) in an isolated yield of 30% (Table 2, entry 1), whereas the (*S*,*R*)/(*R*,*S*) isomers (**21b**) were obtained in 19% yield. As in route 1a, the diastereomers were easily separable using flash column chromatography. We further isolated a by-product in 24% yield, which was identified as another Pictet–Spengler product with the same mass as the desired product. Since the fraction of the by-product was an inseparable mixture of diastereomers, exact identification was not possible, but most likely it is a

**Table 2** Route 1b: Conditions for synthesis of seco-bisbenzylisoquinoline **21**

| Entry | Solvent | Acid | Temperature (°C) | Ratio (*S*,*S*)/(*R*,*R*) : (*S*,*R*)/(*R*,*S*) | Product/by-product |
|---|---|---|---|---|---|
| 1 | DCM | TFA | rt | 62 : 38 | 68 : 32 |
| 2 | DCM | TFA | −15 | 66 : 34 | 66 : 34 |
| 3 | DCM | TfOH | rt | 47 : 53 | 69 : 31 |
| 4 | TFE | TFA | rt | 54 : 46 | 80 : 20 |

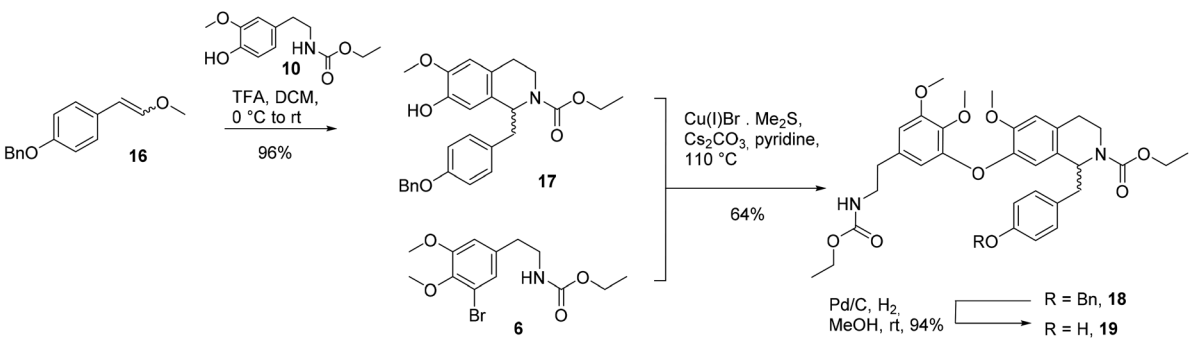


**Scheme 4** Route 1b: Synthesis of diaryl ether **19**.

regioisomer of seco-bisbenzylisoquinoline **21**, resulting from cyclization to the other free *ortho* position of precursor **19**. In order to decrease the amount of this by-product and to improve the diastereomeric ratio we performed the *N*-acyl Pictet–Spengler reaction under different conditions (Table 2). Conducting the reaction at lower temperature (entry 2) had only minor influence in terms of diastereomeric ratio and the formation of the by-product. Using trifluoromethanesulfonic acid (TfOH) instead of TFA (entry 3) increased the formation of (*S*,*R*)/(*R*,*S*) isomers, leading to a more balanced ratio of 47 : 53, but did not decrease by-product formation. Following Kayhan's approach[46] we conducted the reaction in the more polar solvent trifluoroethanol (entry 4), ending up with an improved regioselectivity of 80 : 20. A diastereomeric ratio of 54 : 46 was obtained hereby for the desired regioisomer **21**. Even though the regioselectivity was best in this entry, due to a slow and incomplete conversion we decided to follow our established protocol (entry 1) for the synthesis of seco-bisbenzylisoquinoline **21** (Scheme 5).

In the following step the macrocycle **15** was generated *via* intramolecular C–O coupling of **21** (with previously separated racemic diastereomers) using our protocol as described above, yielding 51% of macrocyclic (*R*,*R*)/(*S*,*S*) isomers (**15a**) and 35% of (*S*,*R*)/(*R*,*S*) isomers (**15b**). Both of these products can be reduced to racemic tetrandrine (*rac*-**1**) and racemic isotetrandrine (*rac*-**2**), respectively, in almost quantitative yields, as shown for route 1a (Scheme 3).

As expected and discussed above, both routes 1a and 1b gave mixtures of diastereomers. Fortunately, chromatographic separation of late intermediates was achieved in both routes, so both racemic tetrandrine (*rac*-**1**) and racemic isotetrandrine (*rac*-**2**) are available in pure form with these approaches. Nevertheless, we intended to expand our approach to a protocol with preference for the one or other of the diastereomers. We presumed that altering the sequence of reactions steps, particularly utilizing an *intra*molecular *N*-acyl Pictet–Spengler reaction for ring closure and construction of the second stereocenter, should lead to an asymmetric induction as a result of the influence of the stereochemistry of the already present asymmetric center and pre-organization of the chiral starting material. This aim was achieved in routes 2a and 2b, as elaborated in detail in the following.

In route 2a, employing the established diaryl ether synthesis protocol, phenolic intermediate **12** from route 1a was coupled with 4-bromophenyl enol ether **13** to obtain **22** in 61% yield (Scheme 6). Next we examined reaction conditions for the intramolecular *N*-acyl Pictet–Spengler condensation. The reaction was carried out at different temperatures (Table 3), expecting that the stereochemical outcome might be controlled by the reaction temperature to a certain extent. We observed no conversion below −20 °C using TFA as catalyst (entry 1). At −20 °C, catalyzed by TFA, macrocycle **15** was formed in 13% yield under predominant formation of the (*R*,*R*)/(*S*,*S*) isomers **15a** (diastereomeric ratio dr 84 : 16; entry 2), hence favouring

**Table 3** Conditions for cyclization *via* *N*-acyl Pictet–Spengler condensation

| Entry | Temperature (°C) | Acid | Ratio (*R*,*R*)/(*S*,*S*) : (*S*,*R*)/(*R*,*S*) | Yield (%) |
|---|---|---|---|---|
| 1 | −78 to −25 | TFA | — | — |
| 2 | −20 | TFA | 84 : 16 | 13 |
| 3 | −15 | TFA | 87 : 13 | 28 |
| 4 | 20 | TFA | 82 : 18 | 25 |
| 5 | −78 | TfOH | 78 : 22 | 9 |
| 6 | 40 | *p*-TsOH | 62 : 38 | >5 |

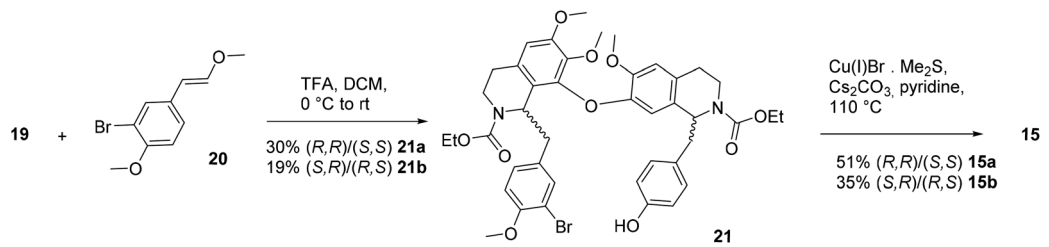


**Scheme 5** Route 1b: Synthesis of seco-bisbenzylisoquinoline **21** and cyclization.

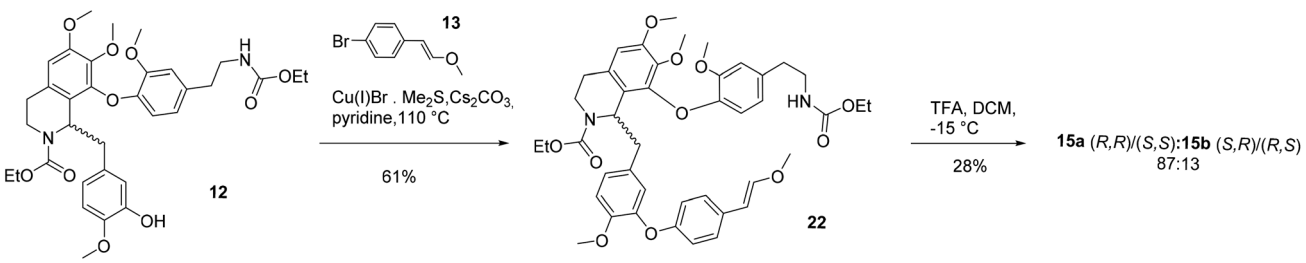


**Scheme 6** Route 2a: Cyclization *via* intramolecular Pictet–Spengler condensation.

 

the relative stereoconfiguration of tetrandrine (**1**) (*S*,*S*) and its enantiomer phaeanthine (*R*,*R*). The best result was obtained at −15 °C (entry 3) in terms of diastereomeric ratio (87 : 13) and yield (28%). When performing the reaction at ambient temperature we obtained a comparable yield (25%) and a d.r. of 82 : 18 (entry 4). With the stronger acid trifluoromethanesulfonic acid (TfOH) macrocycle **15** was generated even at −78 °C, but in a very poor yield of 9% in a 78 : 22 ratio (entry 5). With toluenesulfonic acid (*p*-TsOH) no noteworthy reaction was observed below 40 °C, and at elevated temperature only inferior dr and poor yield were obtained (entry 6). Eventhough the cyclization step of route 2b suffers from low yield, the asymmetric induction in this step is remarkable and prompted us to do further investigations.

Route 2a involved late stage construction of the tetrahydroisoquinoline moiety (rings A′ + B′) forming the stereocenter at C-1′, but the same concept can also be applied to C-1 in ring B. So, in route 2b, we used the same building blocks as in route 1b, but performed the Ullmann coupling first, followed by an intramolecular Pictet–Spengler reaction. Diaryl ether **23** was obtained from phenolic intermediate **19** and brominated enol ether **20** employing the established diaryl ether synthesis protocol in a yield of 43%. Important for this step is the use of freshly synthesized enol ether **20**, since it tends to decompose quickly resulting in minor yields. In attempts to improve this yield we once again examined Pd-catalysts (compare entry 2 in Table 1), but obtained only traces of the desired product **23**. In the subsequent intramolecular Pictet–Spengler reaction, catalyzed by TFA at −15 °C, macrocycle **15** (see Scheme 3) was obtained in 79% yield, but in strong contrast to route 2a, here the isotetrandrine-type (*S*,*R*)/(*R*,*S*) isomers **15b** were formed predominantly in a ratio of 71 : 29 (determined by HPLC) (Scheme 7). In contrast to route 1b, where regioisomeric products were obtained in intermolecular Pictet–Spengler reactions, we detected exclusively the desired cyclization products in this intramolecular reaction. Whereas route 2a does not provide an advantage over route 1a in terms of yield, the access of isotetrandrine-type isomers in route 2b could be improved compared to route 2a.

Final step of both routes 2a and 2b was, as in routes 1a and 1b, the reduction of both ethyl carbamate moieties in **15** using $LiAlH_4$ in THF to give *N*-methyl groups, ending up with mixtures of racemic tetrandrine (*rac*-**1**) and racemic isotetrandrine (*rac*-**2**) (see Scheme 3). Separation of these diastereomers is possible using preparative TLC[47] or preparative HPLC, so pure racemic alkaloids can also be obtained *via* routes 2a and 2b.

In Inubushi's synthetic approach,[28] which included an intramolecular Bischler–Napieralski reaction, some stereocontrol was also observed, but in this case the second stereocenter was not built up in the course of the cyclization reaction, but in the following reduction of the formed 3,4-dihydroisoquinoline moiety to the corresponding tetrahydroisoquinoline. The best dr obtained there was 4 : 1 (determined by NMR). In terms of yields our synthesis is superior to Inubushi's approach. The diaryl ethers in our synthesis were obtained in yields of 41–64%, whereas Inubushi yielded 42–48% (according to the information given in the Experimental section[28]). Tetrahydroisoquinoline units were generated in yields of 47–96% in one single step *via* *N*-acyl Pictet–Spengler condensations here, whereas Inubushi's Bischler–Napieralski protocol with subsequent reduction of the dihydroisoquinolines furnished the corresponding tetrahydroisoquinolines in yields of 28–35% over three steps. Furthermore, the Bischler–Napieralski method requires arylacetic acid precursors which are mostly laborious to access. The enol ethers required in our synthetic approach are easily obtained in a single step in excellent yields from commercially available and cheap benzaldehydes.

In summary we have established a new total synthesis of racemic tetrandrine (*rac*-**1**) and racemic isotetrandrine (*rac*-**2**) in a total of 12 steps in all routes (compared to more than 20 steps in Inubushi's total synthesis[27]). The overall yields of both alkaloids taken together when combining the building blocks **6**, **7**, **10** and **13** are 10.5% in route 1a and 3.0% in route 2a. In route 1b the overall yield amounts 12.4% and in route 2b 19.2% after combination of the building blocks **6**, **10**, **16** and **20**. Compared to the overall yield of 2.1% in Inubushi's approach (as well starting from corresponding building blocks) our synthetic method is up to nine times more efficient. Whereas routes 1a and 1b provide almost equimolar, separable mixtures of both diastereomeric forms (*rac*-**1** and *rac*-**2**), the routes involving *intra*molecular *N*-acyl Pictet–Spengler condensations show good stereoselectivity for the one or other diastereomer. Since the stereoselectivity in our approach is limited, the synthesis of enantiomerically pure bisbenzylisoquinoline alkaloids based on our work remains part

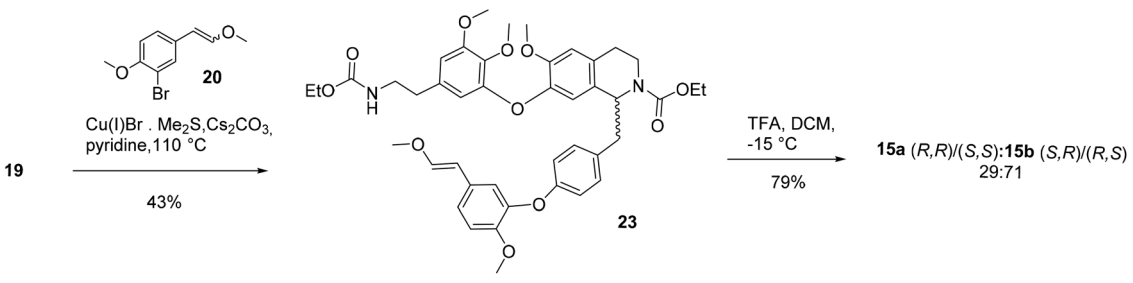


Scheme 7 Route 2b: Alternative cyclization *via* intramolecular *N*-acyl Pictet–Spengler condensation.

of future projects. As numerous protocols have been published for the synthesis of enantiomerically pure monomeric 1-benzyltetrahydroisoquinolines,[48–56] further elaboration of such building blocks using our protocols could provide enantiomerically pure bisbenzylisoquinolines as well.

To understand the surprisingly different diastereomeric outcome of the routes 2a and 2b, we performed an *in silico* conformational analysis of the macrocyclic intermediate structures formed during the crucial intramolecular Pictet–Spengler condensation of **22** (route 2a) and **23** (route 2b). The initial step of these cyclizations is the reaction of the protonated enol ether building block with the arylethylamine-derived carbamate, giving rise to a macrocyclic *N*-acyl iminium ion (and a carbenium ion mesomeric structure) as the reactive intermediate, which then will build up the new stereocenter at C-1 (or C-1′) by electrophilic attack at C-8a (or C-8a′) of the aromatic ring. The putative cationic intermediates of routes 2a and 2b are depicted in Fig. 3 (routes 1a and 1b, in which cyclization occurs after the formation of both stereocenters, did not lead to any (route 1a) or a satisfactory (route 1b) selectivity). Important for selectivity is the construction of the macrocycle under formation of the second stereocenter in one reaction step.

To investigate all aspects of this complex reaction on a quantitative level a two-step workflow would be necessary. First, the evaluation of the stability of different conformations of the macrocyclic intermediates by molecular mechanics-based sampling techniques to identify possible starting conformations for the final reaction step. Second, the investigation of the reaction pathway of this following final reaction step using quantum mechanics-based methods, which reveal *e.g.* the energetic barriers and, thus, the reactivity of the selected starting conformations. Subsequently combining structural data of the first step with the corresponding energetics of the second step can provide a mechanistic as well as the energetic explanation of the experimental results. Nevertheless, as reaction pathway calculations are very demanding, they are normally performed only for the "final" reaction pathway, *i.e.* the one which was experimentally found to perform best. Thus, the corresponding calculations are either done to explain details of the reaction mechanism or to investigate the basic underlying reaction mechanism if it is unknown. However, they are not practically applicable (*i.e.* too computationally demanding) for investigating differences in the outcome of alternative reaction routes, as in this case the reaction pathways for all investigated routes would have to be calculated. As the major goal of our computational studies was to provide a molecular explanation for exactly such differences, we asked ourselves if a stability analysis of the macrocyclic intermediates based on conformational sampling (*e.g.* the first step, see above) could already be helpful for such analysis. One necessary prerequisite for this to be true would be that the results obtained from such simulations correlate well with the experimentally observed final diastereometric ratios. In this context it needs to be stated that, as no reaction pathways are calculated, a computational analysis of reaction-related quantities as *e.g.* the experimentally observed racemic nature of the final reaction products would not be possible based on such studies.

Therefore, to investigate the above question, we practically conducted extensive molecular dynamics simulations of both isomers of the macrocyclic intermediates formed during the reaction routes 2a and 2b and then compared the outcome of our simulations to the diastereomeric ratios for tetrandrine and isotetrandrine as obtained experimentally for those pathways. The applied computational setup was based on a protocol specifically established and afterwards applied successfully for simulating macrocyclic compounds in the context of molecular docking,[57–59] where a similar analysis of conformational ensembles of macrocyclic-ring conformations from molecular dynamics simulations in solution was found to represent the conformational space very well providing that the simulation time and conditions are chosen properly (for a detailed description of the sampling conditions see Computational details). For this the Amber16[60] software was used with General Amber Force Field[61] parameters for all intermediate structures with point charges derived according to the general guidelines for RESP charges (see Computational details for more technical information). Both intermediate structures of route 2a (2b) were simulated as carbenium ions containing a single bond between N-2′ (N-2) and C-1′ (C-1) (highlighted bonds in Fig. 3). This mesomeric form was chosen as it allows for free rotation around that bond, which we rationalized to be the most realistic representation for our purpose as the potential configuration around the second stereocenter to be built up at C-1′ (C-1) is not biased by structural inflexibility in that

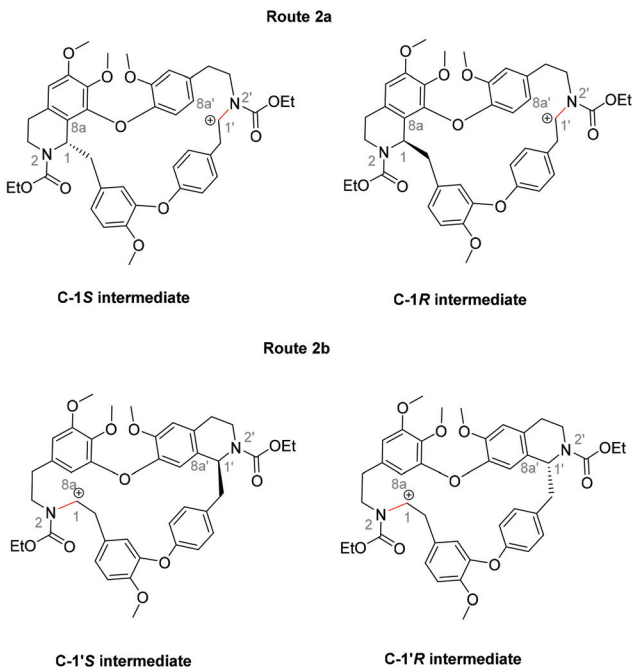


**Fig. 3** Structures of the macrocyclic intermediates of the reactions **22** → **15** (route 2a) and **23** → **15** (route 2b).

region. This would have been the case for the putative iminium mesomeric form, *i.e.* the explicit simulation of *E*- and *Z*-isomers. Thus the structural ensembles obtained from the long-term simulations of the four intermediate structures (Fig. 3) contain pre-reaction conformers of all possible intermediates formed previous to the cyclization step of routes 2a and 2b. Afterwards, these ensembles were geometrically analyzed to, first, evaluate if there exists indeed a correlation between these conformational ensembles and the experimental diastereometric ratios, and second, provide a system-specific structural explanation of the observed selectivities.

Therefore, we focused on two points during the analysis: first, to evaluate how high the probability for each intermediate is to form a pre-reactive structure which, from a geometrical point of view, allows the reaction to occur, and second, to analyze which configuration is the most probable to be formed at the second stereocenter, depending on the conformation of the sampled intermediates. Therefore, we concentrated on a detailed structural analysis of the obtained pre-reactive conformational ensembles, focusing on the 1–2 (1′–2′) bond (highlighted in red in Fig. 3) and the adjacent aromatic ring A (A′), as their spatial orientation was found to be important for the potential configuration of the second stereocenter, as discussed hereinafter. This analysis reveals the probability of the macrocyclic scaffold being oriented towards a specific outcome and can therefore be linked to the likelihood of product formation. Accordingly, the diastereomeric ratio could be assessed computationally by combining all conformers with similar sets of potential configurations previous to the crucial cyclization step.

For each reaction, both isomeric forms of the intermediates (Fig. 3) were investigated. For this, molecular dynamics simulations were performed for all four intermediates under experimental conditions (Table 3, entry 3) and the conformational space of the structures was analyzed. The first 150 conformations featuring a short distance between atoms C-1′ and C-8a′ (C-1 and C-8a for route 2b) were extracted as these structures represent ensembles of possible starting structures for the cyclization step of the *N*-acyl Pictet–Spengler condensation. These sets of conformations were further analyzed (see computational details at the end of this article) with respect to their spatial orientation of C-1 (or C-1′) in relation to the position of ring A (or ring A′), which initiates the nucleophilic attack under construction of the second stereocenter. Respective structures will be called "pre-reaction" ensembles or conformations in the further discussion.

Table S1‡ lists the summarized results of the overall conformational analysis of the first 150 structures of the pre-reaction ensembles. From the simulations of intermediates of route 2a 34 conformers of C-1*R* intermediates and 87 of the C-1*S* intermediates are likely to form *S*-configuration at the second stereocenter being built (referred as "pre-*S*"), whereas 24 of the C-1*R* intermediates and 5 of the C-1*S* intermediates can be expected to form a *R*-configured second stereocenter (referred as "pre-*R*"). Combining this data of both intermediates with respect to the total amount of 150 pre-reaction conformations results in a computational diastereomeric ratio of 74% : 26% tetrandrine : isotetrandrine ((*S*,*S*)/(*R*,*R*) : (*S*,*R*)/(*R*,*S*)) as listed in Table 4. The same analysis performed for the intermediates of route 2b led to 44 conformations of the C-1′*R* intermediate and 30 of the C-1′*S* intermediate conformations showing pre-*S* orientation, whereas 28 of C-1′*R* and 48 of C-1′*S* intermediates can be assigned to pre-*R* for the second stereocenter. Therefore, a computational ratio of 39% : 61% tetrandrine : isotetrandrine ((*S*,*S*)/(*R*,*R*) : (*S*,*R*)/(*R*,*S*)) could be obtained computationally (Table 4).

**Table 4** Summary table listing observed experimental and estimated computational ratios deduced from and colour coded according to values in Table S1‡ based on geometrical analysis of the first 150 (all) conformations of the pre-reaction ensembles

| Products | Computational ratio | experimental ratio |
|---|---|---|
| Route 2a (**22** → **15**) (*S*,*S*)/(*R*,*R*) : (*S*,*R*)/(*R*,*S*) | 74 : 26 (71 : 29) | 87 : 13 |
| Route 2b (**23** → **15**) (*S*,*S*)/(*R*,*R*) : (*S*,*R*)/(*R*,*S*) | 39 : 61 | 29 : 71 |

In contrast to route 2b, where comparable proportions of conformations are sampled for the pre-organized enantiomers, the C-1*S* intermediate of route 2a shows surprisingly high preference of adopting a conformation favouring pre-*S* orientation at the second stereocenter – which is absent for the enantiomeric counterpart (C-1*R* oriented towards C-1′ pre-*R*). Considering the enantiomeric nature of the intermediates, these results are unfortunately not as it is to be expected. Although a reliable prediction of the stereochemical outcome for solely one enantiomeric intermediate in route 2a with our computational analysis is therefore limited, the average ratio of the combined data of both C-1*S* and C-1*R* intermediates reproduces the experimentally observed ratio very well (87% : 13% tetrandrine : isotetrandrine (*S*,*S*)/(*R*,*R*) : (*S*,*R*)/(*R*,*S*)). However, to minimize and investigate any potential impact of insufficient sampling, four additional replicas were simulated for both intermediates of route 2a, such that finally a total of 547 pre-reaction conformations could be extracted from all combined trajectories and the above analysis was repeated for the larger pre-reaction ensembles (see computational details and values in brackets in Tables 4 and S1‡). The assessed computational ratio for all pre-reaction conformers of route 2a of 71% : 29% tetrandrine : isotetrandrine is very close to the previous one considering only the first 150 conformations (74% : 26%) and shows similar trends for both enantiomers (Table S1‡). Summarizing, the overall final simulation times for route 2a and 2b were 6000 and 4000 ns, respectively. These results show that sufficient sampling was guaranteed and it can be ruled out that the observed preference of the C1-*S* intermediate is due to poor statistics or sampling, which is substantiated by the fact that the potential energy of the C1-*S* intermediates that form pre-*S* configuration on the second stereocenter is on average 16.5 kJ mol$^{-1}$ lower than the one of the C1-*R* intermediate structures obtaining pre-*R* orientation.

The above results show that there exists a very good, qualitative agreement between the average distributions of the pre-reaction ensembles and the measured diastereomeric ratios of routes 2a (87 : 13) and 2b (29 : 71), therefore indicating that the conformational distribution of the cyclic intermediates of this reaction step is correlated to the stereoselectivity of the synthetic pathways 2a and 2b.

Given the good correlation between computational and experimental results, we performed a detailed structural analysis based on geometries of the most prominent structures of the conformational ensembles as depicted in Fig. 4, which were chosen on the basis of the dihedral angle values of the highlighted torsion (data not shown, red in Fig. 3, route 2a: C-1′ and N-2′; route 2b: C-1 and N-2) throughout the simulation. For the pre-reaction ensembles of route 2a, a clear preference towards tetrandrine (*rac*-**1**) was observed (computational product ratio of 74% : 26% (*S*,*S*)/(*R*,*R*) : (*S*,*R*)/(*R*,*S*)), whereas the preference of specific intermediates of route 2b is less pronounced and in contrast to the former with inverted stereochemical preference for the isotetrandrine type (*rac*-**2**) (Tables 4 and S1,‡ computational product ratio of 39% : 61% (*S*,*S*)/(*R*,*R*) : (*S*,*R*)/(*R*,*S*)). Regarding the most dominant conformers of the ensembles, they are characterized by the methoxy group of ring A′ (or the methoxy groups of ring A, respectively) flipped to the front (with respect to the orientation chosen in Fig. 4, A′- (or A-), highlighted in green) if a pre-*S* orientation is observed at the second arising stereocenter and flipped back (A′+ or A+) if it is pre-*R* oriented, which for route 2a leads to the (*S*,*S*)/(*R*,*R*) isomers, *i.e.* to tetrandrine (Fig. 4, top), and to the (*S*,*R*)/(*R*,*S*) isomers for route 2b, *i.e.* to isotetrandrine. In fact, our qualitative analysis shows all pre-reaction conformations originating from both intermediates (C-1*S* and C-1*R*) of route 2a that obtain pre-*R* orientation at the second stereocenter were found in combination with ring A′ flipped to the back (A′+), suggesting a strong correlation between the position of the aromatic ring A′ and the dihedral angle of the highlighted bond (data not shown). Together with the analysis above, the experimentally observed selectivity of route 2a can be explained by the formation of highly stable pre-reaction conformations of the macrocycle. Such a distinct preference is not found for the pre-reaction conformations of route 2b, which agrees with the experimentally observed lower selectivity.

Therefore, according to our in-depth computational analysis, there exists a clear correlation between the conformational ensembles of the cationic macrocyclic intermediates of the cyclization step of routes 2a and 2b in solution and the experimentally determined diastereomeric ratios for both reactions. Moreover, even the experimentally observed more pronounced diastereomeric ratio of macrocycle **15** *via* route 2a (intermedi-

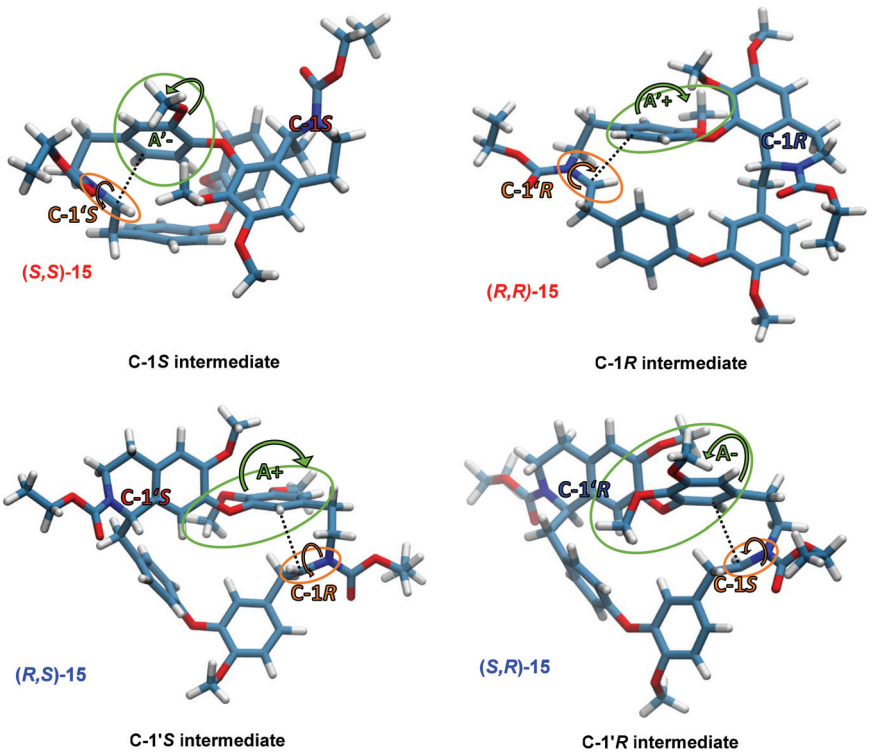


**Fig. 4** Most dominant conformations among the pre-reaction ensembles of macrocyclic cationic intermediate structures of the cyclization step of route 2a (top) and route 2b (bottom), respectively. The structures are characterized by the torsional angle around the highlighted bond (orange) determining the configuration at the newly formed, second stereocenter and the relative position of the aromatic ring (green) and labeled according to the resulting product. The dotted line indicates the final bond formed in this reaction. Atom color scheme: carbon (light blue), nitrogen (dark blue), oxygen (red) and hydrogen (white).

 

ates of **22** → **15**) compared to route 2b (intermediates of **23** → **15**) can be correlated to and thus explained by the relative occurrence of the different pre-reaction conformations sampled. The same holds for the preferred formation of tetrandrine *via* route 2a and isotetrandrine *via* route 2b. Our detailed conformational analysis reveals the structural basis behind these differences: the sampled pre-reaction ensemble of route 2a is dominated by a very stable conformation featuring an optimal geometry for tetrandrine formation. This indicates that in this case the stereochemistry at the first stereocenter at C-1 initiates a structural pre-organization of the macrocyclic ring leading to an optimal orientation for tetrandrine. For route 2b a similarly stable structural pre-arrangement of the macrocyclic ring system cannot be seen and a broader range of conformations is observed in the pre-reaction ensemble, which might explain the lower selectivity of that reaction path.

Although in the current study the computational work was performed after the experiments and only for one specific case study the above results still indicate that – next to explaining the experimental results *a posteriori* – such combined computational/experimental approaches could also be helpful to computationally estimate which synthetic route might be most promising with respect to the desired stereochemical outcome, especially if used in the context of a modular synthesis approach based on established reactions for which the mechanisms and intermediate structures are known in advance. Of course, in such future studies, it would be necessary to re-evaluate on a case-to-case basis which calculated quantities correlate with the desired stereochemical outcome of the synthesis, especially if different reaction types are investigated and in the long run corresponding large-scale benchmark studies need to be performed to establish a generally applicable workflow. In addition, in this context it needs to be stated that considering the low experimental selectivity and the accuracy limits of the used molecular mechanics-based computational methods in the current study, the qualitative reproduction of the diastereomeric trends for both reaction routes is already a very good achievement and any quantitative comparison would go beyond the capability and accuracy of the applied methods. Nevertheless, even on such a qualitative level, similar computational workflows could be helpful in future studies by *e.g.* providing a computational pre-ranking of different possible reactions. This might allow for an *in silico*-guided and thus more efficient experimental investigation of possible reaction pathways.

## Conclusion

By the application of Ullman-type diaryl ether synthesis and *N*-acyl-Pictet–Spengler reactions for the construction of 1-benzyltetrahydroisoquinoline units, especially when employed as central steps in generating the second stereocenter, we could work out a new approach to bisbenzylisoquinoline alkaloids of the tetrandrine (**1**) type, with the perspective for controlling the stereochemical outcome. Having the four different routes presented here in hands, future syntheses of tetrandrine analogues for medicinal chemistry projects can be designed with very high flexibility regarding substitution patterns of all four aromatic rings. In our protocols, any of the four aromatic rings in tetrandrine (**1**)/isotetrandrine (**2**) is derived from a readily available substituted benzaldehyde. Depending on which aromatic ring is subject of intended systematic variations, the corresponding building block can be inserted in a late stage of the synthesis following the best fitting of one of our routes. If stereocontrol is attempted or if all stereoisomers are welcome, the suitable route can be chosen accordingly. So, this work should help to extend the chemical diversity of libraries of analogues bisbenzylisoquinoline alkaloids significantly.

Moreover, with computational approaches we could deliver a reasonable explanation for the observed stereocontrol governing the crucial cyclization step of route 2a. Furthermore, for intramolecular reactions leading to macrocyclic molecules, the combination of theory and experiment as applied herein demonstrates a promising new strategy for optimizing the experimental workflow for the investigation of different possible synthesis pathways. In future, the addition of computational analysis might even enhance the experimental outcome of similar modular synthesis setups, for which the underlying reaction mechanisms and crucial intermediates are known, *e.g.* by estimating diastereomeric ratios in advance. Thus, the introduced method demonstrates a robust guideline towards targeted synthesis.

## Experimental section

### General methods

All solvents and reagents were purchased from commercial suppliers and were used without further purification, unless mentioned otherwise. Anhydrous THF was distilled from sodium/benzophenone under nitrogen atmosphere. TLC was carried out on 0.2 mm silica gel polyester plates with a fluorescence indicator (POLYGRAM SIL G/$UV_{254}$). For preparative TLC 1 mm PLC Silica gel 60 $F_{254}$ plates (20 × 20 cm) with concentrating zone (Merck) were used. Flash chromatography was performed on 40–63 μm silica gel using the solvent systems indicated. NMR spectra were recorded with a 400 MHz (400 MHz for $^{1}H$ and 101 MHz for $^{13}C$), 500 MHz (500 MHz for $^{1}H$ and 126 MHz for $^{13}C$), or 600 MHz Bruker Biospin Avance spectrometer (599 MHz for $^{1}H$ and 151 MHz for $^{13}C$). Peak assignments were based on 2D NMR experiments using standard pulse programs (COSY, HSQC/HMQC, DEPT, HMBC). Chemical shifts were referenced to the residual solvent signal ($CDCl_3$: $\delta_H$ = 7.26 ppm, $\delta_C$ = 77.16 ppm; $CD_3OD$: $\delta_H$ = 3.31 ppm, $\delta_C$ = 49.0 ppm). For the characterization of rotamers a temperature program was employed for recording both 1D and 2D spectra. Hereby chemical shifts were referenced to the signal of tetramethylsilane in deuterated tetrachloroethane ($Tcl_2$ [100 °C]: $\delta_H$ = 5.92 ppm, $\delta_C$ = 74.0 ppm). IR spectra were recorded using a Jasco FT/IR-4100 (type A) instrument equipped with a diamond ATR unit (Jasco PRO450-S). High

resolution mass spectra (HR-MS) were recorded using a Jeol Mstation 700 or JMS GCmate II Jeol instrument for electron impact ionisation (EI). Thermo Finnigan LTQ was used for electrospray ionisation (ESI). HPLC purity was determined using InfinityLab Poroshell 120EC-C18 and 120CN-C18 columns (2.7 μm, 100 × 3.0 mm), detecting at 210 nm and 254 nm. For quantitative analysis of compound **15** and **21** HPLC was performed on a Agilent InfinityLab Poroshell 120 EC-C18 column (2,7 μm, 100 × 3.0 mm) using following method: eluent 50% ACN, 49.9% water and 0.1% THF; flow 0.8 mL $min^{-1}$; temperature 50 °C; Agilent 1100/1200 Diode Array Detector ($\lambda$ = 210 nm). Preparative HPLC was performed on a Macherey-Nagel Nucleodur® 100–5 column (5 μm, 250 × 10 mm) using a VWR LaPrep P110 system with a UV Detector P311.

### General procedure 1: Wittig olefination

A suspension of (methoxymethyl)triphenylphosphonium chloride (1.2 equiv.) in anhydrous THF (2 mL per mmol aromatic aldehyde) was cooled to 0 °C under nitrogen atmosphere. A solution of lithium diisopropylamide (1.4 equiv., 2.0 M solution in THF) was added dropwise and the resulting mixture stirred for 45 min. A solution of the aromatic aldehyde (1.0 equiv.) in anhydrous THF (2 mL per mmol) was added with stirring. The mixture was allowed to warm up to ambient temperature and stirred for 4 h. The reaction was then quenched with deionized water and extracted 3× with ethyl acetate. The combined organic phases were washed with brine, dried over anhydrous $Na_2SO_4$ and concentrated *in vacuo* to afford the crude product which was purified by column chromatography.

### General procedure 2: *N*-acyl Pictet–Spengler condensation

A solution of carbamate (1.0 equiv.) and enol ether (1.2–1.5 equiv.) in dichloromethane (for *inter*molecular reactions 10 mL per mmol carbamate) was cooled to 0 °C under nitrogen atmosphere. Trifluoroacetic acid (10 equiv.) was added dropwise. The reaction was allowed to warm to ambient temperature and stirred for 6–12 h. The intramolecular reactions were conducted at an educt concentration of 0.01 mM and cooled to −15 °C. After adding TFA (10 equiv.) the temperature was kept at −15 °C until the reaction has completed after 12 h. A saturated $NaHCO_3$ solution was then added for neutralization and the aqueous phase extracted 3× with dichloromethane. The combined organic phases were dried over anhydrous $Na_2SO_4$ and concentrated *in vacuo* to afford the crude product which was purified by column chromatography.

### General procedure 3: Ullmann-type C–O coupling reaction

According to a modified procedure of Wang *et al.*,[38] bromoarene (1.0–1.2 equiv.), phenol (1.0–2.0 equiv.), CuBr·$Me_2S$ (1 equiv.) and $Cs_2CO_3$ (3 equiv.) were placed in a pressure tube or a flask closed with a screwcap with septum inlet and sealed with PTFE tape. Anhydrous pyridine (for *inter*molecular C–O coupling reactions 10 mL per mmol bromoarene, for intramolecular reaction a concentration of 0.02 mM was chosen) was added and after 5 min of pre-stirring the reaction was heated to 110 °C for 2–7 days under nitrogen atmosphere. The reaction mixture was concentrated *in vacuo*, diluted with ethyl acetate and filtered over a small plug of silica gel in order to remove the catalyst and the excess base, followed by washing with ethyl acetate. The filtrate was concentrated *in vacuo* to afford a brown oil as crude product which was purified by column chromatography.

### (*E*)-3-Bromo-4,5-dimethoxy-1-(2-nitrovinyl)benzene (4)

Synthesized from 3-bromo-4,5-dimethoxybenzaldehyde (10.5 g, 42.8 mmol) according to the procedure of Maresh *et al.*[33] The crude product was purified by flash column chromatography (50% dichloromethane in hexanes, $R_f$ = 0.25) and the title compound obtained as bright yellow crystalline solid (7.37 g, 25.7 mmol, 60%). Purity (HPLC) = 92% ($\lambda$ = 210 nm). Mp: 153.5 °C. $^1$H NMR, COSY (500 MHz, $CDCl_3$): $\delta$ [ppm] = 7.88 (d, $J$ = 13.6 Hz, 1H, H-1′), 7.51 (d, $J$ = 13.6 Hz, 1H, H-2′), 7.37 (d, $J$ = 2.1 Hz, 1H, H-2), 6.98 (d, $J$ = 2.0 Hz, 1H, H-6), 3.92 (s, 3H, 4-OC$H_3$), 3.92 (s, 3H, 5-OC$H_3$). $^{13}$C NMR, DEPT, HMQC, HMBC (126 MHz, $CDCl_3$): $\delta$ [ppm] = 154.2 (C-5), 149.9 (C-4), 137.7 (C-1′), 137.3 (C-2′), 127.0 (C-1), 126.4 (C-2), 118.7 (C-3), 111.6 (C-6), 61.0 (4-O$CH_3$), 56.4 (5-O$CH_3$). IR (ATR): $\tilde{\nu}$ [$cm^{-1}$] = 2919, 1628, 1414, 1352, 1279, 1151, 1044, 962, 831. HRMS (EI): $m/z$ calcd for $[C_{10}H_{10}BrNO_4]^{\bullet+}$ 286.9788 and 288.9767, found: 286.9801 and 288.9810.

### 3-Bromo-*N*-ethoxycarbonyl-4,5-dimethoxyphenethylamine (6)

Nitrostyrene **4** (7.37 g, 25.7 mmol) was reduced to 3-bromo-4,5-dimethoxyphenethylamine (**5**) following a procedure of Maresh *et al.*[33] The crude product (an orange oil) was dissolved in dichloromethane (100 mL) under nitrogen atmosphere and the solution cooled to 0 °C. Triethylamine (14.1 mL, 101 mmol) was added, followed by ethyl chloroformate (6.06 mL, 63.4 mmol) in a dropwise fashion. The mixture was allowed to warm to ambient temperature and stirred for 14 h, then quenched with saturated $NaHCO_3$ solution (50 mL) and extracted with dichloromethane (3 × 80 mL). The combined organic phases were dried over anhydrous $Na_2SO_4$ and concentrated *in vacuo* to afford a yellow oil. Purification was accomplished by flash column chromatography (dichloromethane, $R_f$ = 0.12) to give **6** as pale yellow oil (5.95 g, 18.0 mmol, 70%). Purity (HPLC) = 100% ($\lambda$ = 210 nm). $^1$H NMR, COSY (400 MHz, $CDCl_3$) $\delta$ [ppm] = 6.96 (d, $J$ = 1.9 Hz, 1H, H-2), 6.69–6.66 (m, 1H, H-6), 4.68 (s, 1H, NH), 4.11 (q, $J$ = 7.1 Hz, 2H, O$CH_2$–$CH_3$), 3.85 (s, 3H, 5-OC$H_3$), 3.83 (s, 3H, 4-OC$H_3$), 3.40 (q, $J$ = 6.8 Hz, 2H, NC$H_2$–$CH_2$), 2.73 (t, $J$ = 7.0 Hz, 2H, $NCH_2$–C$H_2$), 1.23 (t, $J$ = 7.1 Hz, 3H, $OCH_2$–C$H_3$). $^{13}$C NMR, DEPT, HMQC, HMBC (101 MHz, $CDCl_3$) $\delta$ [ppm] = 156.7 (*C*═O), 153.8 (C-5), 145.2 (C-4), 136.2 (C-1), 124.8 (C-2), 117.8 (C-3), 112.4 (C-6), 61.0 (O$CH_2$–$CH_3$), 60.7 (4-O$CH_3$), 56.2 (5-O$CH_3$), 42.1 (N$CH_2$–$CH_2$), 35.9 ($NCH_2$–*C*$H_2$), 14.8 ($OCH_2$–*C*$H_3$). IR (ATR): $\tilde{\nu}$ [$cm^{-1}$] = 3354, 2937, 2826, 1697, 1488, 1271, 1235, 1140, 1044, 1001, 817. HRMS (ESI): $m/z$ calcd for $[C_{13}H_{18}BrNO_4 + H]^+$ 332.0497 and 334.0477, found: 332.0493 and 334.0474.

**(*E*/*Z*)-3-(Benzyloxy)-4-methoxy-1-(2-methoxyvinyl)benzene (7)**

3-Benzyloxy-4-methoxybenzaldehyde (6.01 g, 24.8 mmol) was reacted following General procedure 1 (Wittig olefination). The reaction was completed after 4 h. Purification was accomplished by flash column chromatography (10% ethyl acetate in hexanes, $R_f$ = 0.30) and the product obtained as white solid (yield 5.89 g, 21.8 mmol, 88%). The major product is the *E*-isomer (*E*,*Z*-isomer ratio 1 : 0.82, estimated by NMR-integrals). Purity (HPLC) = 100% ($\lambda$ = 210 nm). Mp: 95.5–96.0 °C. NMR data of the major *E*-isomer: $^1$H NMR, COSY (500 MHz, $CDCl_3$) $\delta$ [ppm] = 7.50–7.43 (m, 2H, H-6-Ph, H-2-Ph), 7.41–7.27 (m, 3H, H-5-Ph, H-4-Ph, H-3-Ph), 6.86 (d, $J$ = 13.1 Hz, 1H, H-2′), 6.84–6.76 (m, 3H, H-2, H-5, H-6), 5.72 (d, $J$ = 12.9 Hz, 1H, H-1′), 5.16 (s, 2H, OC$H_2$-Ph), 3.87 (s, 3H, 4-OC$H_3$), 3.65 (s, 3H, 2′-OC$H_3$). $^{13}$C NMR, DEPT, HMQC, HMBC (126 MHz, $CDCl_3$) $\delta$ [ppm] = 148.2 (C-3), 147.9 (C-4), 147.9 (C-2′), 137.4 (C-1-Ph), 129.4 (C-1), 128.7 (C-5-Ph, C-3-Ph), 128.0 (C-4-Ph), 127.5 (C-6-Ph, C-2-Ph), 118.4 (C-6), 112.4 (C-5), 111.4 (C-2), 104.9 (C-1′), 71.3 (O$CH_2$–Ph), 56.6 (2′-O$CH_3$), 56.3 (4-O$CH_3$). IR (ATR): $\tilde{\nu}$ [cm$^{-1}$] = 3060, 2931, 1638, 1514, 1254, 1134, 1010, 746, 698. HRMS (EI): *m*/*z* calcd for $[C_{17}H_{18}O_3]^{\bullet+}$ 270.1251, found: 270.1251.

**(±)-8-Bromo-*N*-ethoxycarbonyl-6,7-dimethoxy-1-(3′-benzyloxy-4′-methoxybenzyl)-1,2,3,4-tetrahydroisoquinoline (8)**

Carbamate **6** (5.89 g, 17.8 mmol) and enol ether **7** (5.76 g, 21.3 mmol) were condensed following General procedure 2 (for *inter*molecular *N*-acyl Pictet–Spengler reaction) to give tetrahydroisoquinoline **8**. The reaction was completed after 12 h. The crude product was purified by flash column chromatography (20% acetone in hexanes, $R_f$ = 0.17) and the title compound obtained as a pale yellow solid (4.66 g, 8.19 mmol, 46%). Purity (HPLC) = 98% ($\lambda$ = 210 nm). Mp: 40.5–42.5 °C. $^1$H NMR, COSY (400 MHz, $Tcl_2$, 100 °C) $\delta$ [ppm] = 7.46–7.41 (m, 2H, H-6-Ph, H-2-Ph), 7.38–7.32 (m, 2H, H-5-Ph, H-3-Ph), 7.31–7.26 (m, 1H, H-4-Ph), 6.79 (d, $J$ = 8.1 Hz, 1H, H-5′), 6.74 (d, $J$ = 2.0 Hz, 1H, H-2′), 6.70 (dd, $J$ = 8.1, 2.0 Hz, 1H, H-6′), 6.60 (s, 1H, H-5), 5.58–5.48 (m, 1H, H-1), 5.02 (s, 2H, OC$H_2$-Ph), 4.03–3.84 (m, 3H, H-3, OC$H_2$–$CH_3$), 3.83 (s, 3H, 7-OC$H_3$), 3.82 (s, 3H, 6-OC$H_3$), 3.81 (s, 3H, 4′-OC$H_3$), 3.43 (ddd, $J$ = 13.2, 8.8, 5.5 Hz, 1H, H-3), 3.15 (dd, $J$ = 14.3, 3.9 Hz, 1H, H-α), 2.84–2.70 (m, 2H, H-4, H-α), 2.53 (d, $J$ = 13.9 Hz, 1H, H-4), 1.07 (br s, 3H, OC$H_2$–C$H_3$). $^{13}$C NMR, DEPT, HMQC, HMBC (101 MHz, $Tcl_2$, 100 °C) $\delta$ [ppm] = 155.5 (*C*═O), 152.3 (C-6), 149.3 (C-4′), 148.8 (C-3′), 145.7 (C-7), 137.9 (C-1-Ph), 131.7 (C-4a), 131.6 (C-1′), 129.9 (C-8a), 128.4 (C-3-Ph, C-5-Ph), 127.7 (C-4-Ph), 127.5 (C-2-Ph, C-6-Ph), 122.9 (C-6′), 118.3 (C-8), 117.5 (C-2′), 113.7 (C-5′), 112.9 (C-5), 72.0 (O$CH_2$–Ph), 61.2 (O$CH_2$–$CH_3$), 60.5 (7-O$CH_3$), 56.8 (4′-O$CH_3$ or 6-O$CH_3$), 56.5 (4′-O$CH_3$ or 6-O$CH_3$), 56.1 (C-1), 39.1 (C-α), 38.0 (C-3), 28.1 (C-4), 14.5 (OC$H_2$–$CH_3$). IR (ATR): $\tilde{\nu}$ [cm$^{-1}$] = 2934, 2836, 1691, 1596, 1513, 1425, 1318, 1246, 1137, 1101, 1024, 741, 697. HRMS (ESI): *m*/*z* calcd for $[C_{29}H_{32}BrNO_6 + H]^+$ 570.1486 and 572.1465, found: 570.1489 and 572.1471.

***N*-Ethoxycarbonyl-4-hydroxy-3-methoxyphenethylamine (10)**

3-Methoxytyramine hydrochloride (3.46 g, 17.2 mmol) was suspended in dichloromethane (100 mL) under nitrogen atmosphere and the mixture cooled to 0 °C. Triethylamine (9.58 mL, 68.7 mmol) was added, followed by ethyl chloroformate (4.11 mL, 43.0 mmol) in a dropwise fashion. The reaction was allowed to warm to ambient temperature and stirred for 15 h. After this time TLC analysis showed complete conversion to a less polar product ($R_f$ = 0.26, dichloromethane), which is the ethoxycarbonylated phenol intermediate. For chemoselective cleavage of the phenol ester, an ethanolic sodium hydroxide solution (1 M, 100 mL) was added to the reaction and the mixture stirred for 2 h at ambient temperature. After addition of hydrochloric acid (2 M, 60 mL) the organic solvents were removed *in vacuo* and the remaining aqueous solution was extracted with dichloromethane (3 × 100 mL). The combined organic phases were dried over anhydrous $Na_2SO_4$ and concentrated *in vacuo* to afford a beige oil. Purification by flash column chromatography (30% ethyl acetate in hexanes, $R_f$ = 0.20) gave the title compound as a white solid (3.70 g, 15.5 mmol, 90%). Purity (HPLC) = 100% ($\lambda$ = 210 nm). Mp: 95.0–95.5 °C. $^1$H NMR, COSY (400 MHz, $CDCl_3$) $\delta$ [ppm] = 6.84 (d, $J$ = 8.2 Hz, 1H, H-5), 6.70–6.65 (m, 2H, H-6, H-2), 5.62 (s, 1H, O*H*), 4.69 (s, 1H, N*H*), 4.10 (q, $J$ = 7.1 Hz, 2H, OC$H_2$–$CH_3$), 3.86 (s, 3H, OC$H_3$), 3.39 (q, $J$ = 6.7 Hz, 2H, NC$H_2$–$CH_2$), 2.73 (t, $J$ = 7.0 Hz, 2H, NC$H_2$–C$H_2$), 1.22 (t, $J$ = 7.1 Hz, 3H, OC$H_2$–C$H_3$). $^{13}$C NMR, DEPT, HMQC, HMBC (101 MHz, $CDCl_3$) $\delta$ [ppm] = 156.8 (C-3′), 146.7 (C-3), 144.4 (C-4), 130.7 (C-1), 121.5 (C-2), 114.6 (C-5), 111.4 (C-6), 60.9 (O$CH_2$–$CH_3$), 56.0 (O$CH_3$), 42.4 (N$CH_2$–$CH_2$), 35.9 (NC$H_2$–$CH_2$), 14.8 (OC$H_2$–$CH_3$). IR (ATR): $\tilde{\nu}$ [cm$^{-1}$] = 3368, 3273, 1687, 1518, 1237, 1125, 1033, 824, 781. HRMS (ESI): *m*/*z* calcd for $[C_{12}H_{16}NO_4]^-$ 238.1085, found: 238.1087.

**(±)-8-(4-(2-((Ethoxycarbonyl)amino)ethyl)-2-methoxyphenoxy)-*N*-ethoxycarbonyl-6,7-dimethoxy-1-(3′-benzyloxy-4′-methoxybenzyl)-1,2,3,4-tetrahydroisoquinoline (11)**

Tetrahydroisoquinoline **8** (3.00 g, 5.26 mmol) and phenol **10** (2.52 g, 10.5 mmol) were coupled following General Procedure 3 (*inter*molecular Ullmann-type C–O coupling reaction). The reaction was completed after 7 days. Purification was accomplished by flash column chromatography (10% ethyl acetate in dichloromethane, $R_f$ = 0.26) and the product obtained as a beige solid (1.57 g, 2.16 mmol, 41%). Purity (HPLC) = 97% ($\lambda$ = 210 nm). Mp: 58.5–60 °C. $^1$H NMR, COSY (400 MHz, $Tcl_2$, 100 °C) $\delta$ [ppm] = 7.41–7.37 (m, 2H, H-6-Ph, H-2-Ph), 7.36–7.30 (m, 2H, H-5-Ph, H-3-Ph), 7.30–7.25 (m, 1H, H-4-Ph), 6.79 (d, $J$ = 2.0 Hz, 1H, H-2″), 6.73 (d, $J$ = 8.1 Hz, 1H, H-5′), 6.66 (d, $J$ = 2.0 Hz, 1H, H-2′), 6.62–6.59 (m, 1H, H-6′), 6.59–6.57 (m, 1H, H-6″), 6.55 (d, $J$ = 8.2 Hz, 1H, H-5″), 6.50 (s, 1H, H-5), 5.42–5.32 (m, 1H, H-1), 4.92 (s, 2H, OC$H_2$–Ph), 4.56 (s, 1H, N*H*), 4.07 (q, $J$ = 7.1 Hz, 2H, ‘OC$H_2$–$CH_3$), 4.03–3.92 (m, 1H, H-3), 3.89 (s, 3H, 3″-OC$H_3$), 3.81 (s, 3H, 6-OC$H_3$), 3.91–3.69 (m, 2H, OC$H_2$–$CH_3$), 3.78 (s, 3H, 4′-OC$H_3$), 3.60 (s, 3H, 7-OC$H_3$), 3.36 (q, $J$ = 6.9 Hz, 2H, NC$H_2$–$CH_2$), 3.33–3.25 (m, 1H, H-3), 3.13 (dd, $J$ = 14.0, 3.8

Hz, 1H, H-α), 2.80 (dd, $J$ = 14.1, 9.0 Hz, 2H, H-4, H-α), 2.72 (t, $J$ = 7.1 Hz, 2H, $NCH_2$–$CH_2$), 2.50 (d, $J$ = 16.4 Hz, 1H, H-4), 1.20 (t, $J$ = 7.1 Hz, 3H, '$OCH_2$–$CH_3$), 0.93 (br s, 3H, $OCH_2$–$CH_3$). $^{13}$C NMR, DEPT, HMQC, HMBC (101 MHz, $Tcl_2$, 100 °C) $\delta$ [ppm] = 156.5 ('*C*═O), 155.4 (*C*═O), 152.6 (C-6), 149.5 (C-3″), 149.0 (C-4′), 148.7 (C-3′), 146.9 (C-4″), 145.4 (C-8), 140.6 (C-7), 137.9 (C-1-Ph), 133.3 (C-1″), 132.3 (C-1′), 130.3 (C-4a), 128.4 (C-5-Ph, C-3-Ph, 127.7 (C-4-Ph), 127.6 (C-6-Ph, C-2-Ph), 124.2 (C-8a), 122.9 (C-6′), 121.0 (C-6″), 117.4 (C-2′), 115.6 (C-5″), 114.7 (C-2″), 113.6 (C-5′), 109.6 (C-5), 71.8 ($OCH_2$–Ph), 60.9 ($OCH_2$–$CH_3$), 60.7 ('$OCH_2$–$CH_3$), 60.7 (7-$OCH_3$), 56.9 (4′-$OCH_3$ or 3″-$OCH_3$), 56.8 (4′-$OCH_3$ or 3″-$OCH_3$), 56.4 (6-$OCH_3$), 52.1 (C-1), 42.3 ($NCH_2$–$CH_2$), 39.9 (C-α), 37.7 (C-3), 35.9 ($NCH_2$–$CH_2$), 28.1 (C-4), 14.6 ('$OCH_2$–$CH_3$), 14.4 ($OCH_2$–$CH_3$). IR (ATR): $\tilde{\nu}$ [$cm^{-1}$] = 2936, 2832, 1690, 1606, 1509, 1424, 1330, 1255, 1212, 1154, 1131, 1108, 1069, 1023, 758. HRMS (ESI): $m/z$ calcd for $[C_{41}H_{48}N_2O_{10} + H]^+$ 729.3382, found: 729.3385.

### (±)-8-(4-(2-((Ethoxycarbonyl)amino)ethyl)-2-methoxyphenoxy)-*N*-ethoxycarbonyl-6,7-dimethoxy-1-(3′-hydroxy-4′-methoxybenzyl)-1,2,3,4-tetrahydroisoquinoline (12)

To a solution of diaryl ether **11** (1.00 g, 1.37 mmol) in methanol (50 mL) palladium (10% on carbon, 100 mg, Pd 0.094 mmol) was added. The reaction was stirred for 12 h at ambient temperature under hydrogen atmosphere (1 atm). The catalyst was removed by passing the mixture through a small plug of Celite, followed by washing with methanol (50 mL). The filtrate was concentrated *in vacuo* to give a white solid (0.805 g, 1.26 mmol, 92%) as desired product with no side products. The isolated product was used without purification for the following Pictet–Spengler cyclization. Purity (HPLC) = 99% ($\lambda$ = 210 nm). Mp: 61.5–62.0 °C. $^1$H NMR, COSY (400 MHz, $Tcl_2$, 100 °C) $\delta$ [ppm] = 6.81 (d, $J$ = 2.0 Hz, 1H, H-2″), 6.66 (d, $J$ = 8.2 Hz, 1H, H-5′), 6.61 (d, $J$ = 2.1 Hz, 1H, H-2′), 6.57 (dd, $J$ = 8.2, 2.0 Hz, 1H, H-6″), 6.52 (d, $J$ = 8.2 Hz, 1H, H-5″), 6.52–6.48 (m, 2H, H-5, H-6′), 5.42 (s, 1H, O*H*), 5.36 (dd, $J$ = 9.4 Hz, 1H, H-1), 4.64 (s, 1H, N*H*), 4.07 (q, $J$ = 7.1 Hz, 2H, '$OCH_2$–$CH_3$), 4.08–3.94 (m, 1H, H-3), 3.92 (s, 3H, 3″-$OCH_3$), 3.82 (s, 3H, 6-$OCH_3$), 3.79 (s, 3H, 4′-$OCH_3$), 3.87–3.66 (m, 2H, $OCH_2$–$CH_3$), 3.61 (s, 3H, 7-$OCH_3$), 3.37 (q, $J$ = 7.0 Hz, 2H, $NCH_2$–$CH_2$), 3.39–3.28 (m, 1H, H-3), 3.10 (dd, $J$ = 14.0, 3.8 Hz, 1H, H-α), 2.89–2.78 (m, 1H, H-4), 2.79–2.70 (m, 1H, H-α), 2.73 (t, $J$ = 7.0 Hz, 2H, $NCH_2$–$CH_2$), 2.59 (d, $J$ = 16.4 Hz, 1H, H-4), 1.20 (t, $J$ = 7.1 Hz, 3H, '$OCH_2$–$CH_3$), 0.92 (br s, 3H, $OCH_2$–$CH_3$). $^{13}$C NMR, DEPT, HMQC, HMBC (101 MHz, $Tcl_2$, 100 °C) $\delta$ [ppm] = 156.5 ('*C*═O), 155.4 (*C*═O), 152.6 (C-6), 149.5 (C-3″), 146.7 (C-4″), 145.5 (C-8), 145.4 (C-4′), 145.3 (C-3′), 140.7 (C-7), 133.2 (C-1″), 132.6 (C-1′), 130.1 (C-4a), 124.4 (C-8a), 121.0 (C-6′), 120.8 (C-6″), 116.1 (C-2′), 115.4 (C-5″), 114.4 (C-2″), 111.1 (C-5′), 109.8 (C-5), 60.9 ($OCH_2$–$CH_3$), 60.7 (7-$OCH_3$, '$OCH_2$–$CH_3$, 56.7 (3″-$OCH_3$), 56.4 (6-$OCH_3$ or 4′-$OCH_3$), 56.3 (6-$OCH_3$ or 4′-$OCH_3$), 52.0 (C-1), 42.3 ($NCH_2$–$CH_2$), 39.8 (C-α), 37.5 (C-3), 35.9 ($NCH_2$–$CH_2$), 28.0 (C-4), 14.6 ('$OCH_2$–$CH_3$), 14.2 ($OCH_2$–$CH_3$). IR (ATR): $\tilde{\nu}$ [$cm^{-1}$] = 3354, 2939, 1686, 1594, 1508, 1419, 1331, 1244, 1211, 1129, 1109, 1023, 960, 761. HRMS (ESI): $m/z$ calcd for $[C_{34}H_{41}N_2O_{10}]^-$ 637.2767, found: 637.2785.

### (*E*/*Z*)-4-Bromo-1-(2-methoxyvinyl)benzene (13)

Prepared from 4-bromobenzaldehyde (2.00 g, 10.8 mmol) following General procedure 1 (Wittig olefination). Purification was accomplished by flash column chromatography (2.5% ethyl acetate in hexanes, $R_f$ = 0.23/0.30) to give the title compound as a colourless oil (2.06 g, 9.72 mmol, 90%, *E*,*Z*-isomer ratio 1 : 0.85, estimated by NMR integrals). Purity (HPLC) = 76% ($\lambda$ = 210 nm). $^1$H NMR, COSY (400 MHz, $CDCl_3$) *E*-isomer: $\delta$ [ppm] = 7.40–7.35 (m, 2H, H-3, H-5), 7.11–7.07 (m, 2H, H-2, H-6), 7.03 (d, $J$ = 13.0 Hz, 1H, H-2′), 5.74 (d, $J$ = 13.0 Hz, 1H, H-1′), 3.68 (s, 3H, $OCH_3$). $^{13}$C NMR, DEPT, HMQC, HMBC (101 MHz, $CDCl_3$) *E*-isomer: $\delta$ [ppm] = 149.5 (C-2′), 135.5 (C-1), 131.3 (C-3, C-5), 126.8 (C-2, C-6), 119.1 (C-4), 104.2 (C-1′), 56.7 ($OCH_3$). IR (ATR): $\tilde{\nu}$ [$cm^{-1}$] = 2929, 2832, 1589, 1488, 1405, 1120, 1069, 1010, 816. HRMS (EI): $m/z$ calcd for $[C_9H_9BrO]^{\bullet+}$ 211.9831 and 213.9811, found: 211.9827 and 213.9806.

### (±)-8-((1-(4-Bromobenzyl)-*N*-(ethoxycarbonyl)-6-methoxy-1,2,3,4-tetrahydroisoquinolin-7-yl)oxy)-*N*-ethoxycarbonyl-6,7-dimethoxy-1-(3′-hydroxy-4′-methoxybenzyl)-1,2,3,4-tetrahydroisoquinoline (14) (separable mixture of racemic diastereomers)

Carbamate **12** (600 mg, 0.939 mmol) and enol ether **13** (240 mg, 1.13 mmol) were condensed following General procedure 2 (*inter*molecular *N*-acyl Pictet–Spengler reaction). The reaction was completed after 12 h. For separation of the racemic diastereomers of **14** 15% ethyl acetate in dichloromethane ($R_f$ = 0.21 for the (1*R*,1′*R*)/(1*S*,1′*S*) isomers (**14a**) and 0.30 for the (1*R*,1′*S*)/(1*S*,1′*R*) isomers (**14b**)) was used.

(1*R*,1′*R*)/(1*S*,1′*S*) isomers **14a**: Yield: (385 mg, 0.471 mmol, 50%). Purity (HPLC) = 92% ($\lambda$ = 210 nm). Mp: 73.0–75.0 °C. $^1$H NMR, COSY (400 MHz, $Tcl_2$, 100 °C) $\delta$ [ppm] = $\delta$ 7.23–7.18 (m, 2H, H-13′, H-11′), 6.86–6.80 (m, 2H, H-14′, H-10′), 6.70 (s, 1H, H-5′), 6.67 (d, $J$ = 8.1 Hz, 1H, H-13), 6.63 (d, $J$ = 2.0 Hz, 1H, H-10), 6.55 (s, 1H, H-5), 6.50 (dd, $J$ = 8.2, 2.1 Hz, 1H, H-14), 6.22 (s, 1H, H-8′), 5.35 (s, 2H, H-1, O*H*), 5.05 (t, $J$ = 6.3 Hz, 1H, H-1′), 4.13–4.04 (m, 1H, H-3), 4.01 (q, $J$ = 7.1 Hz, 2H, '$OCH_2$–$CH_3$), 3.97–3.89 (m, 1H, H-3′), 3.91 (s, 3H, 6′-$OCH_3$), 3.85 (s, 3H, 6-$OCH_3$), 3.87–3.66 (m, 2H, $OCH_2$–$CH_3$), 3.80 (s, 3H, 12-$OCH_3$), 3.61 (s, 3H, 7-$OCH_3$), 3.40–3.30 (m, 1H, H-3), 3.23–3.12 (m, 1H, H-3′), 2.98 (dd, $J$ = 14.0, 3.6 Hz, 1H, H-α), 2.92–2.81 (m, 1H, H-4), 2.86 (dd, $J$ = 6.4, 3.5 Hz, 2H, H-α′), 2.81–2.73 (m, 1H, H-4′), 2.70 (dd, $J$ = 13.9, 10.0 Hz, 1H, H-α), 2.62 (d, $J$ = 16.3 Hz, 1H, H-4), 2.53 (dt, $J$ = 16.0, 4.6 Hz, 1H, H-4′), 1.14 (t, $J$ = 7.1 Hz, 3H, '$OCH_2$–$CH_3$), 0.92 (br s, 3H, $OCH_2$–$CH_3$). $^{13}$C NMR, DEPT, HMQC, HMBC (101 MHz, $Tcl_2$, 100 °C) $\delta$ [ppm] = 155.4 (*C*═O), ('*C*═O), 152.5 (C-6), 148.4 (C-6′), 146.2 (C-7′), 145.5 (C-11), 145.4 (C-12), 145.0 (C-8), 140.6 (C-7), 137.4 (C-9′), 132.6 (C-9), 131.2 (C-14′, C-10′), 131.1 (C-13′, C-11′), 130.0 (C-4a), 128.8 (C-8a′), 128.3 (C-4a′), 124.3 (C-8a), 121.0 (C-14), 120.2 (C-12′), 116.0 (C-10), 114.0 (C-8′), 113.7 (C-5′), 111.0 (C-13), 110.1 (C-5), 61.2 ('$OCH_2$–$CH_3$), 60.9 ($OCH_2$–$CH_3$), 60.7 (7-$OCH_3$), 56.6 (6′-$OCH_3$), 56.5 (6-$OCH_3$), 56.4 (12-$OCH_3$), 55.6 (C-1′), 52.0 (C-1), 42.6 (C-α′), 39.8 (C-α), 38.9 (C-3′), 37.3 (C-3), 28.2 (C-4′), 28.0 (C-4), 14.6 ('$OCH_2$–$CH_3$), 14.2 ($OCH_2$–$CH_3$). IR (ATR): $\tilde{\nu}$ [$cm^{-1}$] = 3527, 2923, 2853, 1686, 1607,

 

1508, 1426, 1330, 1237, 1196, 1120, 1068, 1024, 804, 760. HRMS (ESI): *m*/*z* calcd for $[C_{42}H_{47}BrN_2O_{10} + H]^+$ 819.2487 and 821.2466, found: 819.2479 and 821.2460.

(1*R*,1′*S*)/(1*S*,1′*R*) isomers **14b**: Yield: (354 mg, 0.433 mmol, 46%). Purity (HPLC) = 96% ($\lambda$ = 210 nm). Mp: 89.0–90.0 °C. $^1$H NMR, COSY (400 MHz, $Tcl_2$, 100 °C) $\delta$ [ppm] = 7.24–7.18 (m, 2H, H-13′, H-11′), 6.88–6.82 (m, 2H, H-14′, H-10′), 6.69 (s, 1H, H-5′), 6.68 (d, *J* = 2.1 Hz, 1H, H-10), 6.67 (d, *J* = 8.2 Hz, 1H, H-13), 6.55 (s, 1H, H-5), 6.53 (dd, *J* = 8.4, 1.9 Hz, 1H, H-14), 6.16 (s, 1H, H-8′), 5.38 (s, 1H, O*H*), 5.32 (dd, *J* = 9.7, 3.2 Hz, 1H, H-1), 5.03 (t, *J* = 6.2 Hz, 1H, H-1′), 4.13–3.93 (m, 4H, H-3, H-3′, ‘OC*H*$_2$–CH$_3$), 3.90 (s, 3H, 6′-OC*H*$_3$), 3.84 (s, 3H, 6-OC*H*$_3$), 3.86–3.74 (m, 2H, OC*H*$_2$–CH$_3$), 3.80 (s, 3H, 12-OC*H*$_3$), 3.62 (s, 3H, 7-OC*H*$_3$), 3.42–3.31 (m, 1H, H-3), 3.22–3.08 (m, 2H, H-α, H-3′), 2.98–2.87 (m, 1H, H-4), 2.85 (dd, *J* = 6.3, 3.4 Hz, 2H, H-α′), 2.84–2.71 (m, 2H, H-α, H-4′), 2.64 (d, *J* = 16.2 Hz, 1H, H-4), 2.53 (dt, *J* = 16.0, 4.4 Hz, 1H, H-4′), 1.14 (t, *J* = 7.1 Hz, 3H, ‘OCH$_2$–C*H*$_3$), 0.95 (br s, 3H, OCH$_2$–C*H*$_3$). $^{13}$C NMR, DEPT, HMQC, HMBC (101 MHz, $Tcl_2$, 100 °C) $\delta$ [ppm] = 155.4 (*C*═O, ‘*C*═O), 152.4 (C-6), 148.3 (C-6′), 146.1 (C-7′), 145.5 (C-8), 145.4 (C-12), 145.0 (C-11), 140.7 (C-7), 137.6 (C-9′), 132.6 (C-9), 131.2 (C-14′, C-10′), 131.1 (C-13′, C-11′), 130.0 (C-4a), 128.9 (C-8a′), 128.1 (C-4a′), 124.2 (C-8a), 121.1 (C-14), 120.1 (C-12′), 116.1 (C-10), 113.6 (C-5′, C-8′), 111.0 (C-13), 110.2 (C-5), 61.2 (‘O*C*H$_2$–CH$_3$), 60.9 (O*C*H$_2$–CH$_3$), 60.7 (7-O*C*H$_3$), 56.6 (6-O*C*H$_3$ or 6′-O*C*H$_3$), 56.5 (6-O*C*H$_3$ or 6′-O*C*H$_3$), 56.3 (12-O*C*H$_3$), 55.7 (C-1′), 52.0 (C-1), 42.7 (C-α′), 39.8 (C-α), 38.7 (C-3′), 37.5 (C-3), 28.3 (C-4′), 28.1 (C-4), 14.6 (‘OCH$_2$–*C*H$_3$), 14.3 (OCH$_2$–*C*H$_3$). IR (ATR): $\tilde{\nu}$ [cm$^{-1}$] = 3438, 2931, 2840, 1692, 1609, 1510, 1427, 1332, 1237, 1201, 1122, 1069, 1026, 804, 760. HRMS (ESI): *m*/*z* calcd for $[C_{42}H_{47}BrN_2O_{10} + H]^+$ 819.2487 and 821.2466, found: 819.2480 and 821.2461.

### (±)-*N*,*N*′-Bis-(ethoxycarbonyl)-nortetrandrine and isomers (15)

*Method A* – Preparation by cyclization *via* intramolecular Ullmann-type C–O coupling reaction:

Previously separated diastereomers of bisbenzylisoquinoline **14** (200 mg, 0.244 mmol of pure diastereomer) or of bisbenzylisoquinoline **21**, respectively (200 mg, 0.244 mmol of pure diastereomer) were reacted following General Procedure 3 (intramolecular C–O coupling). The reactions were completed after 52 h. Purification was accomplished by flash column chromatography (35% acetone in hexanes, $R_f$ = 0.29) and the products obtained as beige solids.

Yields obtained from bisbenzylisoquinoline **14a**: (1*R*,1′*R*)/(1*S*,1′*S*) isomers: 115 mg, 0.156 mmol, 64%; (1*R*,1′*S*)/(1*S*,1′*R*) isomers: 112 mg, 0.152 mmol, 62%.

Yields obtained from bisbenzylisoquinoline **21a**: (1*R*,1′*R*)/(1*S*,1′*S*) isomers: 91.9 mg, 0.124 mmol, 51%; (1*R*,1′*S*)/(1*S*,1′*R*) isomers: 63.1 mg, 0.0854 mmol, 35%.

*Method B* – Preparation by intramolecular *N*-acyl Pictet–Spengler reaction:

Enol ether **22** or enol ether **23**, respectively (50.0 mg, 0.0649 mmol) were reacted following General procedure 2 (intramolecular *N*-acyl Pictet–Spengler reaction). The reactions were completed after 12 h. Purification was accomplished by flash column chromatography (35% acetone in hexanes, $R_f$ = 0.29). Yield obtained from enol ether **22**: 13.5 mg, 0.0183 mmol, 28%; yield obtained from enol ether **23**: 38.0 mg, 0.0514 mmol, 79%.

(1*R*,1′*R*)/(1*S*,1′*S*) isomers **15a**: Purity (HPLC) = 94% ($\lambda$ = 210 nm). Mp 132–134 °C. $^1$H NMR, COSY (400 MHz, $Tcl_2$, 100 °C) $\delta$ [ppm] = 7.38 (d, *J* = 8.2 Hz, 1H, H-14′ or H-10′), 7.12 (dd, *J* = 8.2, 2.5 Hz, 1H, H-13′ or H-11′), 6.79 (d, *J* = 8.1 Hz, 1H, H-13), 6.67 (s, 1H, H-13′ or H-11′), 6.64 (s, 1H, H-5′), 6.56 (dd, *J* = 8.1, 2.0 Hz, 1H, H-14), 6.47 (d, *J* = 1.9 Hz, 1H, H-10), 6.32 (s, 1H, H-5), 6.19 (dd, *J* = 8.4, 2.2 Hz, 1H, H-14′ or H-10′), 6.16 (s, 1H, H-8′), 5.26 (t, *J* = 6.1 Hz, 1H, H-1), 5.04 (s, 1H, H-1′), 4.36–4.20 (m, 3H, H-3, ‘OC*H*$_2$–CH$_3$), 4.03–3.95 (m, 1H, H-3′), 3.87 (s, 3H, 12-OC*H*$_3$), 3.73 (s, 3H, 6-OC*H*$_3$), 3.89–3.59 (m, 2H, OC*H*$_2$–CH$_3$), 3.53–3.37 (m, 3H, H-3, H-3′, H-α′), 3.34 (s, 3H, 6′-OC*H*$_3$), 3.26 (s, 3H, 7-OC*H*$_3$), 3.19–3.07 (m, 1H, H-4′), 2.94–2.75 (m, 2H, H-4, H-4′), 2.71 (d, *J* = 5.9 Hz, 2H, H-α), 2.69–2.59 (m, 2H, H-4, H-α′), 1.36 (t, *J* = 7.1 Hz, 3H, ‘OCH$_2$–C*H*$_3$), 0.86 (br s, 3H, OCH$_2$–C*H*$_3$). $^{13}$C NMR, DEPT, HMQC, HMBC (101 MHz, $Tcl_2$, 100 °C) $\delta$ [ppm] = 155.9 (‘*C*═O), 155.6 (*C*═O), 154.3 (C-12′), 152.0 (C-6), 150.2 (C-11), 149.1 (C-6′), 147.9 (C-12), 147.0 (C-8), 144.9 (C-7′), 138.9 (C-7), 134.6 (C-9′), 133.8 (C-9), 132.2 (C-14′ or C-10′), 130.1 (C-14′ or C-10′), 130.0 (C-4a′), 128.8 (C-8a′), 128.1 (C-4a), 122.9 (C-8a), 122.0 (C-13′ or C-11′), 121.9 (C-14), 121.5 (C-13′ or C-11′), 119.6 (C-8′), 116.8 (C-10), 114.1 (C-5′), 113.6 (C-13), 107.4 (C-5), 61.4, (‘O*C*H$_2$–CH$_3$), 60.7 (O*C*H$_2$–CH$_3$), 60.3 (7-O*C*H$_3$), 57.7 (C-1′), 57.1 (12-O*C*H$_3$ or 6′-O*C*H$_3$), 57.0 (12-O*C*H$_3$ or 6′-O*C*H$_3$), 56.3 (6-O*C*H$_3$), 53.5 (C-1), 41.9 (C-3′, C-α′), 40.9 (C-α), 36.6 (C-3), 28.0 (C-4), 27.8 (C-4′), 14.8 (‘OCH$_2$–*C*H$_3$), 14.2 (OCH$_2$–*C*H$_3$). IR (ATR): $\tilde{\nu}$ [cm$^{-1}$] = 2940, 2832, 1687, 1585, 1507, 1417, 1330, 1277, 1252, 1230, 1207, 1123, 1097, 1024, 841, 768. HRMS (ESI): *m*/*z* calcd for $[C_{42}H_{46}N_2O_{10} + H]^+$ 739.3225, found: 739.3223.

(1*R*,1′*S*)/(1*S*,1′*R*) isomers **15b**: Purity (HPLC) = 95% ($\lambda$ = 210 nm). Mp 142.5–144.0 °C. $^1$H NMR, COSY (400 MHz, $Tcl_2$, 100 °C) $\delta$ [ppm] = 7.40–7.33 (m, 1H, H-14′ or H-10′), 7.07 (dd, *J* = 8.2, 2.5 Hz, 1H, H-13′ or H-11′), 6.76 (d, *J* = 8.0 Hz, 1H, H-13), 6.66–6.60 (m, 2H, 5′, H-13′ or H-11′), 6.57 (dd, *J* = 8.0, 2.0 Hz, 1H, H-14), 6.42–6.36 (m, 1H, H-14′ or H-10′), 6.32 (s, 1H, H-10), 6.28 (s, 1H, H-5), 6.17 (s, 1H, H-8′), 5.26 (d, *J* = 8.7 Hz, 1H, H-1), 5.10 (dd, *J* = 10.5, 6.2 Hz, 1H, H-1′), 4.33–4.07 (m, 3H, H-3, ‘OC*H*$_2$–CH$_3$), 3.96–3.89 (m, 1H, H-3′), 3.87 (s, 3H, 12-OC*H*$_3$), 3.85–3.77 (m, 2H, OC*H*$_2$–CH$_3$), 3.73 (s, 3H, 6-OC*H*$_3$), 3.61 (s, 3H, 6′-OC*H*$_3$), 3.57–3.42 (m, 2H, H-3′, H-α′), 3.38–3.25 (m, 1H, H-3), 3.16 (s, 3H, 7-OC*H*$_3$), 3.15–3.08 (m, 2H, H-α, H-4′), 2.82 (dt, *J* = 15.8, 4.7 Hz, 1H, H-4′), 2.77–2.67 (m, 2H, H-4, H-α′), 2.55 (dd, *J* = 13.9, 9.5 Hz, 1H, H-α), 2.50–2.35 (m, 1H, H-4), 1.33 (t, *J* = 7.1 Hz, 3H, ‘OCH$_2$–C*H*$_3$), 1.00 (br s, 3H, OCH$_2$–C*H*$_3$). $^{13}$C NMR, HSQC, HMBC (101 MHz, $Tcl_2$, 100 °C) $\delta$ [ppm] = 155.8 (*C*═O), 155.5 (‘*C*═O), 154.4 (C-12′), 152.5 (C-6), 150.4 (C-11), 150.1 (C-6′), 147.9 (C-12), 144.4 (C-7′), 137.9 (C-7), 134.8 (C-9′), 134.0 (C-9), 131.5 (C-14′ or C-10′), 130.4 (C-4a′), 130.0 (C-14′ or C-10′), 129.6 (C-4a), 128.3 (C-8a′), 122.1 (C-14, C-13′ or 11′), 122.0 (C-13′ or C-11′), 120.6 (C-8a), 119.6 (C-8′), 117.1 (C-10), 113.3 (C-13), 111.9 (C-5′), 106.9 (C-5), 61.3 (‘O*C*H$_2$–CH$_3$), 60.9 (O*C*H$_2$–CH$_3$), 60.5 (7-O*C*H$_3$), 57.1

(12-O*C*H$_3$), 1′, 56.3 (6-O*C*H$_3$), 56.1 (6′-O*C*H$_3$), 54.1 (C-1), 41.7 (C-3′), 41.6 (C-α′), 39.0 (C-α), 28.2 (C-4), 28.1 (C-4′), 14.8 ('OCH$_2$–*C*H$_3$), 14.3 (OCH$_2$–*C*H$_3$). The resonances of C-3 and C-8 could not be identified. IR (ATR): $\tilde{\nu}$ [cm$^{-1}$] = 2929, 2839, 1693, 1584, 1505, 1417, 1330, 1276, 1255, 1231, 1204, 1124, 1101, 1020, 842, 770. HRMS (ESI): *m*/*z* calcd for [$C_{42}H_{46}N_2O_{10}$ + H]$^+$ 739.3225, found: 739.3225.

### (*E*/*Z*)-4-(Benzyloxy)-1-(2-methoxyvinyl)benzene (16)

Obtained from 4-benzyloxybenzaldehyde (5.00 g, 23.6 mmol) following General Procedure 1 (Wittig olefination). Purification by flash column chromatography (5% ethyl acetate in hexanes, $R_f$ = 0.32) gave the title compound as a white solid (5.50 g, 22.9 mmol, 97%, *E*,*Z*-isomer ratio 1 : 1.4, estimated by NMR-integrals). Purity (HPLC) = 96% ($\lambda$ = 210 nm). Mp: 37.5 °C. NMR data of the major *Z*-isomer: $^1$H NMR, COSY (400 MHz, $CDCl_3$) $\delta$ [ppm] = 7.55–7.48 (m, 2H, H-6, H-2), 7.46–7.41 (m, 2H, H-2-Ph, H-6-Ph), 7.41–7.35 (m, 2H, H-3-Ph, H-5-Ph), 7.35–7.29 (m, 1H, H-4-Ph), 6.93–6.87 (m, 2H, H-3, H-5), 6.06 (d, *J* = 7.0 Hz, 1H, H-2′), 5.18 (d, *J* = 7.0 Hz, 1H, H-1′), 5.06 (s, 2H, OC*H*$_2$–Ph), 3.76 (s, 3H, OC*H*$_3$). $^{13}$C NMR, DEPT, HMQC, HMBC (101 MHz, $CDCl_3$): $\delta$ [ppm] = 156.9 (C-4), 146.6 (C-2′), 137.3 (C-1-Ph), 129.5 (C-6, C-2), 129.2 (C-1), 128.7 (C-3-Ph, C-5-Ph), 128.0 (C-4-Ph), 127.6 (C-2-Ph, C-6-Ph), 114.8 (C-3, C-5), 105.3 (C-1′), 70.1 (O*C*H$_2$–Ph), 60.6 (O*C*H$_3$). IR (ATR): $\tilde{\nu}$ [cm$^{-1}$] = 3034, 2834, 2080, 1639, 1606, 1236, 1093, 836, 739. HRMS (EI): *m*/*z* calcd for [$C_{16}H_{16}O_2$]$^{\bullet+}$ 240.1145, found: 240.1140.

### (±)-*N*-Ethoxycarbonyl-7-hydroxy-6-methoxy-1-(4′-benzyloxybenzyl)-1,2,3,4-tetrahydroisoquinoline (17)

Carbamate **10** (0.950 g, 3.97 mmol) and enol ether **16** (1.43 g, 5.96 mmol) were condensed following General procedure 2 (*inter*molecular *N*-acyl Pictet–Spengler reaction). The reaction was completed after 12 h. Purification by flash column chromatography (5% ethyl acetate in dichloromethane, $R_f$ = 0.29) gave **17** as a white solid (1.71 g, 3.81 mmol, 96%). Purity (HPLC) = 99% ($\lambda$ = 210 nm). Mp: 45.5–48.0 °C. $^1$H NMR, COSY (400 MHz, $Tcl_2$, 100 °C) $\delta$ [ppm] = 7.41–7.37 (m, 2H, H-2-Ph, H-6-Ph), 7.37–7.31 (m, 2H, H-3-Ph, H-5-Ph), 7.30–7.25 (m, 1H, H-4-Ph), 7.00–6.94 (m, 2H, H-2′, H-6′), 6.88–6.83 (m, 2H, H-3′, H-5′), 6.58–6.52 (m, 2H, H-8, H-5), 5.33 (s, 1H, O*H*), 5.14 (t, *J* = 6.7 Hz, 1H, H-1), 5.02 (s, 2H, OC*H*$_2$–Ph), 4.04–3.88 (m, 3H, H-3, OC*H*$_2$–CH$_3$), 3.84 (s, 3H, 6-OC*H*$_3$), 3.22 (ddd, *J* = 13.7, 9.9, 4.6 Hz, 1H, H-3), 2.97 (d, *J* = 6.6 Hz, 2H, H-α), 2.76 (ddd, *J* = 15.9, 9.9, 5.9 Hz, 1H, H-4), 2.51 (dt, *J* = 15.8, 4.4 Hz, 1H, H-4), 1.10 (t, *J* = 7.1 Hz, 3H, OCH$_2$–C*H*$_3$). $^{13}$C NMR, HSQC, HMBC (101 MHz, $Tcl_2$, 100 °C) $\delta$ [ppm] = 157.8 (C-4′), 155.5 (C-7), 145.7 (C-6), 144.1 (*C*═O), 137.6 (C-1-Ph), 131.1 (C-1′), 130.6 (C-2′, C-6′), 130.0 (C-8a), 128.5 (C-3-Ph, C-5-Ph), 127.8 (C-4-Ph), 127.4 (C-2-Ph, C-6-Ph), 126.1 (C-4a), 115.2 (C-3′, C-5′), 113.4 (C-8), 111.3 (C-5), 70.5 (O*C*H$_2$–Ph), 61.1 (O*C*H$_2$–CH$_3$), 56.3 (6-O*C*H$_3$), 56.1 (C-1), 42.1 (C-α), 38.5 (C-3), 28.2 (C-4), 14.6 (OCH$_2$–*C*H$_3$). IR (ATR): $\tilde{\nu}$ [cm$^{-1}$] = 3032, 2929, 2360, 1683, 1509, 1428, 1232, 1201, 1098, 1014, 696. HRMS (ESI): *m*/*z* calcd for [$C_{27}H_{29}NO_5$ + H]$^+$ 448.2118, found: 448.2120.

### (±)-7-(5-(2-((Ethoxycarbonyl)amino)ethyl)-2,3-dimethoxyphenoxy)-*N*-ethoxycarbonyl-6-methoxy-1-(4′-benzyloxybenzyl)-1,2,3,4-tetrahydroisoquinoline (18)

Phenol intermediate **17** (1.70 g, 3.80 mmol) and aryl bromide **6** (1.51 g, 4.56 mmol) were coupled following General procedure 3 (*inter*molecular C–O coupling reaction). The reaction was completed after 3 days. Purification by flash column chromatography (30% acetone in hexanes, $R_f$ = 0.30) affording the product as a beige solid (1.69 g, 2.42 mmol, 64%). Purity (HPLC) = 100% ($\lambda$ = 210 nm). Mp: 46.5–48.0 °C. $^1$H NMR, COSY (400 MHz, $Tcl_2$, 100 °C) $\delta$ [ppm] = 7.40–7.36 (m, 2H, H-2-Ph, H-6-Ph), 7.33 (t, *J* = 7.3 Hz, 2H, H-3-Ph, H-5-Ph), 7.30–7.24 (m, 1H, H-4-Ph), 6.94–6.90 (m, 2H, H-2′, H-6′), 6.82–6.77 (m, 2H, H-3′, H-5′), 6.68 (s, 1H, H-5), 6.50 (s, 1H, H-8), 6.45 (d, *J* = 1.9 Hz, 1H, H-2″), 6.20 (d, *J* = 1.9 Hz, 1H, H-6″), 5.12 (t, *J* = 6.5 Hz, 1H, H-1), 4.98 (s, 2H, OC*H*$_2$–Ph), 4.49 (s, 1H, N*H*), 4.04 (q, *J* = 7.1 Hz, 2H, 'OC*H*$_2$–CH$_3$), 4.03–3.92 (m, 3H, H-3, OC*H*$_2$–CH$_3$), 3.83 (s, 3H, 3″-OC*H*$_3$), 3.79 (s, 3H, 4″-OC*H*$_3$), 3.78 (s, 3H, 6-OC*H*$_3$), 3.30 (q, *J* = 6.8 Hz, 2H, NC*H*$_2$–CH$_2$), 3.23 (ddd, *J* = 13.6, 9.7, 4.6 Hz, 1H, H-3), 2.94 (tt, *J* = 13.7, 7.2 Hz, 2H, H-α), 2.81 (ddd, *J* = 15.8, 9.7, 5.9 Hz, 1H, H-4), 2.64 (t, *J* = 7.1 Hz, 2H, NCH$_2$–C*H*$_2$), 2.61–2.52 (m, 1H, H-4), 1.18 (t, *J* = 7.1 Hz, 3H, 'OCH$_2$–C*H*$_3$), 1.13 (t, *J* = 7.0 Hz, 3H, OCH$_2$–C*H*$_3$). $^{13}$C NMR, HSQC, HMBC (101 MHz, $Tcl_2$, 100 °C) $\delta$ [ppm] = 157.8 (C-4′), 156.4 ('*C*═O), 155.5 (*C*═O), 154.0 (C-3″), 151.1 (C-5″), 149.9 (C-6), 144.4 (C-7), 139.0 (C-4″), 137.5 (C-1-Ph), 134.1 (C-1″), 130.8 (C-1′), 130.6 (C-2′, C-6′), 130.5 (C-8a), 129.8 (C-4a), 128.5 (C-3-Ph, C-5-Ph), 127.8 (C-4-Ph), 127.4 (C-2-Ph, C-6-Ph), 119.0 (C-8), 115.1 (C-3′, C-5′), 114.1 (C-5), 111.5 (C-6″), 108.6 (C-2″), 70.5 (O*C*H$_2$–Ph), 61.2 (O*C*H$_2$–CH$_3$), 60.9 (4″-O*C*H$_3$), 60.7 ('O*C*H$_2$–CH$_3$), 56.7 (3″-O*C*H$_3$), 56.6 (6-O*C*H$_3$), 55.9 (C-1), 42.2 (N*C*H$_2$–CH$_2$), 42.1 (C-α), 38.5 (C-3), 36.2 (NCH$_2$–*C*H$_2$), 28.4 (C-4), 14.6 ('OCH$_2$–*C*H$_3$, OCH$_2$–*C*H$_3$). IR (ATR): $\tilde{\nu}$ [cm$^{-1}$] = 2923, 2849, 1686, 1583, 1508, 1424, 1231, 1102, 1012, 824, 764, 736. HRMS (ESI): *m*/*z* calcd for [$C_{40}H_{46}N_2O_9$ + H]$^+$ 699.3276, found: 699.3277.

### (±)-7-(5-(2-((Ethoxycarbonyl)amino)ethyl)-2,3-dimethoxyphenoxy)-*N*-ethoxycarbonyl-6-methoxy-1-(4′-hydroxybenzyl)-1,2,3,4-tetrahydroisoquinoline (19)

To a solution of diaryl ether **18** (1.69 g, 2.42 mmol) in methanol (50 mL) palladium (10% on carbon, 169 mg, Pd 1.59 mmol) was added. The mixture was stirred for 12 h at ambient temperature under hydrogen atmosphere (1 atm). The catalyst was removed by filtration through a small plug of Celite, followed by washing with methanol (50 mL). The filtrate was concentrated *in vacuo*. Purification by flash column chromatography (35% acetone in hexanes, $R_f$ = 0.22) gave the title compound as a white solid (1.38 g, 2.27 mmol, 94%). Purity (HPLC) = 100% ($\lambda$ = 210 nm). Mp: 63.0–65.5 °C. $^1$H NMR, COSY (400 MHz, $Tcl_2$, 100 °C) $\delta$ [ppm] = 6.85–6.80 (m, 2H, H-2′, H-6′), 6.68 (s, 1H, H-5), 6.66–6.62 (m, 2H, H-3′, H-5′), 6.45 (d, *J* = 1.9 Hz, 1H, H-2″), 6.30 (s, 1H, H-8), 6.19 (d, *J* = 1.9 Hz, 1H, H-6″), 5.49 (s, 1H, O*H*), 5.04 (t, *J* = 6.6 Hz, 1H, H-1), 4.61 (t, *J* = 5.7 Hz, 1H, N*H*), 4.08 (q, *J* = 7.1 Hz, 4H, OC*H*$_2$–CH$_3$,

'OC$H_2$–$CH_3$), 3.95–3.85 (m, 1H, H-3), 3.84 (s, 3H, 3″-O$CH_3$), 3.78 (s, 3H, 6-O$CH_3$), 3.76 (s, 3H, 4″-O$CH_3$), 3.36–3.27 (m, 3H, H-3, NC$H_2$–$CH_2$), 2.99 (dd, $J$ = 13.5, 5.9 Hz, 1H, H-α), 2.86–2.76 (m, 2H, H-4, H-α), 2.68–2.61 (m, 3H, H-4, $NCH_2$–C$H_2$), 1.23–1.17 (m, 6H, $OCH_2$–C$H_3$, '$OCH_2$–C$H_3$). $^{13}$C NMR, HSQC, HMBC (101 MHz, $Tcl_2$, 100 °C) $\delta$ [ppm] = 156.8 ('*C*═O), 155.5 (*C*═O), 154.7 (C-4′), 154.0 (C-3″), 150.8 (C-5″), 149.7 (C-6), 144.7 (C-7), 139.2 (C-4″), 133.9 (C-1″), 130.7 (C-2′, C-6′), 130.1 (C-4a, C-1′), 129.5 (C-8a), 118.6 (C-8), 115.3 (C-3′, C-5′), 114.0 (C-5), 112.2 (C-6″), 108.9 (C-2″), 61.2 ('O*C*$H_2$–$CH_3$ or O*C*$H_2$–$CH_3$), 61.0 ('O*C*$H_2$–$CH_3$ or O*C*$H_2$–$CH_3$), 60.8 (4″-O*C*$H_3$), 56.7 (3″-O*C*$H_3$), 56.6 (6-O*C*$H_3$), 56.3 (C-1), 42.2 (C-α, N*C*$H_2$–$CH_2$), 39.1 (C-3), 36.2 ($NCH_2$–*C*$H_2$), 28.4 (C-4), 14.7 ($OCH_2$*C*$H_3$ or '$OCH_2$*C*$H_3$), 14.6 ($OCH_2$*C*$H_3$ or '$OCH_2$*C*$H_3$). IR (ATR): $\tilde{\nu}$ [$cm^{-1}$] = 2927, 2833, 2362, 1689, 1508, 1425, 1230, 1100, 1007, 773. HRMS (ESI): *m*/*z* calcd for $[C_{33}H_{40}N_2O_9 + H]^+$ 609.2807, found: 609.2810.

### (*E*/*Z*)-3-Bromo-4-methoxy-1-(2-methoxyvinyl)benzene (20)

Obtained from 3-bromo-4-methoxybenzaldehyde (0.500 g, 2.33 mmol) following General Procedure 1 (Wittig olefination). Purification by flash column chromatography (5% ethyl acetate in hexanes, $R_f$ = 0.30) affording the product as a colourless oil (0.455 g, 1.87 mmol, 80%, *E*,*Z*-isomer ratio 1 : 0.91 estimated by NMR-integrals). Purity (HPLC) = 92% ($\lambda$ = 210 nm). NMR data of the major *E*-isomer: $^1$H NMR, COSY (400 MHz, $CDCl_3$) $\delta$ [ppm] = 7.46–7.41 (m, 1H, H-2), 7.11 (dd, $J$ = 8.5, 2.2 Hz, 1H, H-6), 6.93 (d, $J$ = 12.9 Hz, 1H, H-2′), 6.82 (d, $J$ = 5.1 Hz, 1H, H-5), 5.71 (d, $J$ = 12.9 Hz, 1H, H-1′), 3.87 (s, 3H, 4-O$CH_3$), 3.67 (s, 3H, 2′-O$CH_3$). $^{13}$C NMR, DEPT, HMQC, HMBC (101 MHz, $CDCl_3$) $\delta$ [ppm] = 154.1 (C-4), 148.6 (C-2′), 130.7 (C-1), 129.9 (C-2), 125.3 (C-6), 112.3 (C-5), 111.5 (C-3), 103.6 (C-1′), 56.7 (2′-O$CH_3$), 56.5 (4-O$CH_3$). IR (ATR): $\tilde{\nu}$ [$cm^{-1}$] = 2937, 2837, 2074, 1640, 1496, 1253, 1095, 1053, 816. HRMS (EI): *m*/*z* calcd for $[C_{10}H_{11}BrO_2]^{\bullet+}$ 241.9937 and 243.9916, found: 241.9938 and 243.9917.

### (±)-8-((1-(4-Hydroxybenzyl)-*N*-(ethoxycarbonyl)-6-methoxy-1,2,3,4-tetrahydroisoquinolin-7-yl)oxy)-*N*-ethoxycarbonyl-6,7-dimethoxy-1-(3′-bromo-4′-methoxybenzyl)-1,2,3,4-tetrahydroisoquinoline (21) (separable mixture of racemic diastereomers)

Intermediate **19** (200 mg, 0.329 mmol) and enol ether **20** (96.0 mg, 0.394 mmol) were condensed following General Procedure 2 (*inter*molecular *N*-acyl Pictet–Spengler reaction) to give a racemic mixture of diastereomers of tetrahydroisoquinoline **21** in a ratio of 62 : 38 (*R*,*R*)/(*S*,*S*) : (*S*,*R*)/(*R*,*S*). The reaction was completed after 12 h. Purification and separation of the diastereomers was accomplished by flash column chromatography (20% ethyl acetate in dichloromethane, $R_f$ = 0.17 ((1*R*,1′*S*)/(1*S*,1′*R*) isomers (**21b**) and 0.13 (1*R*,1′*R*)/(1*S*,1′*S*) isomers (**21a**)) to give both diasereomers as white solids.

(1*R*,1′*R*)/(1*S*,1′*S*) isomers **21a**: Yield: 113 mg, 0.138 mmol, 42%. Purity (HPLC) = 75% ($\lambda$ = 210 nm). Mp: 68.5–70.5 °C. $^1$H NMR, COSY (400 MHz, $Tcl_2$, 100 °C) $\delta$ [ppm] = 7.18 (d, $J$ = 2.1 Hz, 1H, H-10), 6.91 (dd, $J$ = 8.3, 2.1 Hz, 1H, H-14), 6.81–6.76 (m, 2H, H-14′, H-10′), 6.74–6.68 (m, 2H, H-13, H-5′), 6.58–6.52 (m, 3H, H-5, H-13′, H-11′), 6.21 (s, 1H, H-8′), 5.30 (d, $J$ = 10.1 Hz, 1H, H-1), 5.02 (t, $J$ = 6.5 Hz, 1H, H-1′), 4.86 (s, 1H, O*H*), 4.14–4.04 (m, 1H, H-3), 4.00 (q, $J$ = 7.3 Hz, 2H, 'O*C*$H_2$–$CH_3$), 3.91 (s, 3H, 6′-O*C*$H_3$), 3.96–3.89 (m, 1H, H-3′), 3.85 (s, 3H, 6-O*C*$H_3$), 3.87–3.71 (m, 2H, O*C*$H_2$–$CH_3$), 3.79 (s, 3H, 12-O*C*$H_3$), 3.63 (s, 3H, 7-O*C*$H_3$), 3.37–3.28 (m, 1H, H-3), 3.18 (ddd, $J$ = 13.4, 9.5, 4.4 Hz, 1H, H-3′), 3.05 (dd, $J$ = 14.1, 3.7 Hz, 1H, H-α), 2.88 (d, $J$ = 6.4 Hz, 1H, H-4), 2.84 (t, $J$ = 6.4 Hz, 2H, H-α′), 2.75 (td, $J$ = 16.2, 14.4, 9.9 Hz, 2H, H-α, H-4′), 2.61 (d, $J$ = 6.3 Hz, 1H, H-4), 2.55 (td, $J$ = 11.3, 5.5 Hz, 1H, H-4′), 1.14 (t, $J$ = 7.0 Hz, 3H, '$OCH_2$C$H_3$), 0.89 (br s, 3H, $OCH_2$C$H_3$). $^{13}$C NMR, HSQC, HMBC (101 MHz, $Tcl_2$, 100 °C) $\delta$ [ppm] = 155.5 ('*C*═O), 155.4 (*C*═O), 154.8 (C-12), 154.3 (C-12′), 152.6 (C-6), 148.2 (C-6′), 146.0 (C-7′), 145.0 (C-8), 140.8 (C-7), 134.2 (C-10), 133.2 (C-9), 130.5 (C-14′, C-10′), 130.4 (C-9′), 130.0 (C-8a), 129.4 (C-14), 129.2 (C-8a′), 128.5 (C-4a′), 123.9 (C-4a), 115.3 (C-13′, C-11′), 114.1 (C-8′), 113.5 (C-5′), 112.5 (C-13), 111.7 (C-11), 110.1 (C-5), 61.2 ('O*C*$H_2$–$CH_3$), 61.1 (O*C*$H_2$–$CH_3$), 60.7 (7-O*C*$H_3$), 56.7 (6-, 6′- or 12-O*C*$H_3$), 56.6 (6-, 6′- or 12-O*C*$H_3$), 56.6 (6-, 6′- or 12-O*C*$H_3$), 55.9 (C-1′), 52.0 (C-1), 42.1 (C-α′), 39.2 (C-α), 38.7 (C-3′), 37.4 (C-3), 28.3 (C-4′), 28.0 (C-4), 14.6 ('$OCH_2$*C*$H_3$), 14.2 ($OCH_2$*C*$H_3$). IR (ATR): $\tilde{\nu}$ [$cm^{-1}$] = 2918, 2850, 2366, 1668, 1612, 1497, 1427, 1331, 1255, 1120, 1020, 887, 742. HRMS (ESI): *m*/*z* calcd for $[C_{42}H_{47}BrN_2O_{10} + H]^+$ 819.2492 and 821.2472, found: 819.2500 and 821.2490.

(1*R*,1′*S*)/(1*S*,1′*R*) isomers **21b**: Yield: (70.5 mg, 0.0856 mmol, 26%. Purity (HPLC) = 67% ($\lambda$ = 210 nm). Mp: 71.5–73.5 °C. $^1$H NMR, COSY (400 MHz, $Tcl_2$, 100 °C) $\delta$ [ppm] = 7.24 (d, $J$ = 2.1 Hz, 1H, H-10), 6.94 (dd, $J$ = 8.3, 2.1 Hz, 1H, H-14), 6.77 (d, $J$ = 8.4 Hz, 2H, H-14′, H-10′), 6.74 (d, $J$ = 8.3 Hz, 1H, H-13), 6.70 (s, 1H, H-5′), 6.56 (d, $J$ = 8.3 Hz, 2H, H-13′, H-11′), 6.51 (s, 1H, H-5), 6.11 (s, 1H, H-8′), 5.27 (d, $J$ = 8.3 Hz, 1H, H-1), 5.10 (s, 1H, O*H*), 4.99 (t, $J$ = 6.5 Hz, 1H, H-1′), 4.01 (q, $J$ = 7.1 Hz, 2H, 'O*C*$H_2$–$CH_3$), 4.07–3.89 (m, 2H, H-3, H-3′), 3.90 (s, 3H, 6′-O*C*$H_3$), 3.86–3.78 (m, 2H, O*C*$H_2$–$CH_3$), 3.83 (s, 3H, 6-O*C*$H_3$), 3.80 (s, 3H, 12-O*C*$H_3$), 3.59 (s, 3H, 7-O*C*$H_3$), 3.40–3.31 (m, 1H, H-3′), 3.25 (d, $J$ = 15.6 Hz, 1H, H-3), 3.17 (dd, $J$ = 14.1, 3.9 Hz, 1H, H-α), 2.92–2.73 (m, 5H, H-4, H-α, H-4′, H-α′), 2.62–2.52 (m, 2H, H-4, H-4′), 1.15 (t, $J$ = 7.1 Hz, 3H, '$OCH_2$C$H_3$), 0.97 (br s, 3H, $OCH_2$C$H_3$). $^{13}$C NMR, HSQC, HMBC (101 MHz, $Tcl_2$, 100 °C) $\delta$ [ppm] = 155.6 (═O), 155.5 ('*C*═O), 154.8 (C-12), 154.4 (C-12′), 152.6 (C-6), 148.2 (C-6′), 145.8 (C-7′), 145.2 (C-8), 140.7 (C-7), 134.3 (C-10), 133.2 (C-9), 130.6 (C-14′, C-10′), 130.3 (C-9′), 130.1 (C-4a), 129.5 (C-14), 129.2 (C-8a′), 128.4 (C-4a′), 123.5 (C-8a), 115.3 (C-13′, C-11′), 114.4 (C-8′), 113.4 (C-5′), 112.5 (C-13), 111.7 (C-11), 109.8 (C-5), 61.2 ('O*C*$H_2$–$CH_3$, O*C*$H_2$–$CH_3$), 60.7 (7-O*C*$H_3$), 56.7 (6-, 6′- or 12-O*C*$H_3$), 56.6 (6-, 6′- or 12-O*C*$H_3$), 56.6 (6-, 6′- or 12-O*C*$H_3$), 56.1 (C-1′), 52.1 (C-1), 42.2 (C-α′), 39.4 (C-α) 38.8 (C-3), 37.9 (C-3′), 28.3 (C-4′), 28.1 (C-4), 14.6 ('$OCH_2$*C*$H_3$), 14.4 ($OCH_2$*C*$H_3$). IR (ATR): $\tilde{\nu}$ [$cm^{-1}$] = 2945, 2344, 1686, 1613, 1497, 1431, 1331, 1255, 1120, 1019, 949, 889, 743. HRMS (ESI): *m*/*z* calcd for $[C_{42}H_{47}BrN_2O_{10} + H]^+$ 819.2492 and 821.2472, found: 819.2502 and 821.2493.

### (±)-8-(4-(2-((Ethoxycarbonyl)amino)ethyl)-2-methoxyphenoxy)-*N*-eth-oxycarbonyl-6,7-dimethoxy-1-(4′-methoxy-3′-(4-(2-methoxy-vinyl)phenoxy)benzyl)-1,2,3,4-tetrahydroisoquinoline (22)

Phenol **12** (100 mg, 0.157 mmol) and enol ether **13** (36.7 mg, 0.172 mmol) were coupled following General Procedure 3

(*inter*molecular Ullmann-type C–O coupling reaction). The reaction was completed after 5 days. Purification by flash column chromatography (15% ethyl acetate in dichloromethane, $R_f$ = 0.26) gave **22** as a white solid (74.0 mg, 0.0960 mmol, 61%). Purity (HPLC) = 100% ($\lambda$ = 210 nm). Mp 59.5–61.0 °C. $^1$H NMR, COSY (400 MHz, $Tcl_2$, 100 °C) *Z*-isomer: $\delta$ [ppm] = 7.45–7.38 (m, 1H, H-2‴ or H-6‴), 7.11–7.05 (m, 1H, H-2‴ or H-6‴), 6.86 (d, $J$ = 12.9 Hz, 1H, H-2⁗), 6.81 (d, $J$ = 8.3 Hz, 1H, H-5′), 6.78 (d, $J$ = 2.0 Hz, 1H, H-6′), 6.77–6.71 (m, 3H, H-2″, H-3‴, H-5‴), 6.67 (d, $J$ = 1.9 Hz, 1H, H-2′), 6.55 (dt, $J$ = 8.3, 1.6 Hz, 1H, H-6″), 6.50 (d, $J$ = 8.2 Hz, 1H, H-5″), 6.48 (s, 1H, H-5), 5.80 (d, $J$ = 12.8 Hz, 1H, H-1⁗), 5.32 (d, $J$ = 8.7 Hz, 1H, H-1), 4.58 (s, 1H, N*H*), 4.07 (q, $J$ = 7.1 Hz, 2H, 'OC$H_2$–CH$_3$), 3.97 (d, $J$ = 9.9 Hz, 1H, H-3), 3.91–3.75 (m, 2H, OC$H_2$–CH$_3$), 3.81 (s, 6H, 6-OC$H_3$, 3″-OC$H_3$), 3.72 (s, 3H, 4′-OC$H_3$), 3.64 (s, 3H, 2⁗-OC$H_3$), 3.59 (s, 3H, 7-OC$H_3$), 3.35 (q, $J$ = 6.9 Hz, 2H, NC$H_2$–CH$_2$), 3.32–3.24 (m, 1H, H-3), 3.13 (dd, $J$ = 14.1, 3.9 Hz, 1H, H-α), 2.85–2.73 (m, 2H, H-4, H-α), 2.71 (t, $J$ = 7.1 Hz, 2H, NCH$_2$–C$H_2$), 2.51 (d, $J$ = 16.2 Hz, 1H, H-4), 1.20 (t, $J$ = 7.1 Hz, 3H, 'OCH$_2$–C$H_3$), 0.96 (br s, 3H, OCH$_2$–C$H_3$). $^{13}$C NMR, HSQC, HMBC (101 MHz, $Tcl_2$, 100 °C) *Z*-isomer: $\delta$ [ppm] = 156.5 ('*C*═O), 156.4 (C-4‴), 152.6 (C-6), 150.4 (C-4′), 149.4 (C-3″), 148.1 (C-2⁗), 146.6 (C-4″), 145.1 (C-3′), 140.7 (C-7), 133.2 (C-1″), 132.6 (C-1′), 130.4 (C-1‴), 130.2 (C-4a), 129.4 (C-2‴ or C-6‴), 126.2 (C-2‴ or C-6‴), 125.8 (C-6′), 124.1 (C-8a), 122.8 (C-2′), 120.8 (C-6″), 117.3 (C-3‴ or C-5‴), 116.6 (C-3‴ or C-5‴), 115.4 (C-5″), 114.3 (C-2″), 114.2 (C-5′), 109.7 (C-5), 105.4 (C-1⁗), 61.0 (OC$H_2$–CH$_3$), 60.7 ('OC$H_2$–CH$_3$), 60.4 (7-OC$H_3$), 56.9 (2⁗-OC$H_3$), 56.8 (4′-OC$H_3$), 56.6 (3″-OC*H*3), 56.4 (6-OC$H_3$), 52.1 (C-1), 42.3 (NC$H_2$–CH$_2$), 39.6 (C-α), 37.7 (C-3), 35.9 (NCH$_2$–C$H_2$), 28.0 (C-4), 14.6 ('OCH$_2$–C$H_3$), 14.4 (OCH$_2$–C$H_3$). The resonances of C-8 and *C*═O could not be identified. IR (ATR): $\tilde{\nu}$ [cm$^{-1}$] = 2911, 1693, 1603, 1504, 1423, 1329, 1262, 1213, 1152, 1125, 1108, 1026, 839, 766. HRMS (ESI): $m/z$ calcd for $[C_{43}H_{50}N_2O_{11} + H]^+$ 771.3487, found: 771.3497.

### (±)-7-(5-(2-((Ethoxycarbonyl)amino)ethyl)-2,3-dimethoxyphenoxy)-*N*-ethoxycarbonyl-6-methoxy-1-(4′-(2-methoxy-5-(2-methoxyvinyl)phenoxy)benzyl)-1,2,3,4-tetrahydroisoquinoline (23)

Phenol intermediate **19** (200 mg, 0.329 mmol) and enol ether **20** (87.9 mg, 0.361 mmol) were coupled following General Procedure 3 (*inter*molecular Ullmann-type C–O coupling reaction). The reaction was completed after 48 h. Purification by flash column chromatography (15% ethyl acetate in dichloromethane, $R_f$ = 0.23) affording the product as a beige solid (114 mg, 0.141 mmol, 43%). Purity (HPLC) = 85% ($\lambda$ = 210 nm). Mp: 47.0–50.5 °C. $^1$H NMR, COSY (400 MHz, $Tcl_2$, 100 °C) $\delta$ [ppm] = 6.95–6.84 (m, 4H, H-5‴, H-6‴, H-2′, H-6′), 6.81–6.74 (m, 4H, H-2‴, H-3′, H-5′, H-2⁗), 6.68 (s, 1H, H-5), 6.56 (s, 1H, H-8), 6.46 (s, 1H, H-2″), 6.21 (s, 1H, H-6″), 5.71 (d, $J$ = 12.8 Hz, 1H, H-1⁗), 5.14 (s, 1H, H-1), 4.51 (s, 1H, N*H*), 4.04 (q, $J$ = 7.1 Hz, 2H, 'OC$H_2$–CH$_3$), 4.04–3.90 (m, 3H, 3, OC$H_2$–CH$_3$), 3.84 (s, 3H, 3″-OC$H_3$), 3.80 (s, 3H, 4″-OC$H_3$), 3.78 (s, 3H, 6-OC$H_3$), 3.73 (s, 3H, 4‴-OC$H_3$), 3.60 (s, 3H, 2⁗-OC$H_3$), 3.30 (q, $J$ = 6.9 Hz, 2H, NC$H_2$–CH$_2$), 3.27–3.18 (m, 1H, H-3), 2.95 (d, $J$ = 6.6 Hz, 2H, H-α), 2.81 (ddd, $J$ = 16.0, 9.5, 6.6 Hz, 1H, H-4), 2.64 (t, $J$ = 7.1 Hz, 2H, NCH$_2$–C$H_2$), 2.61–2.52 (m, 1H, H-4), 1.17 (t, $J$ = 7.1 Hz, 3H, 'OCH$_2$C$H_3$), 1.13 (t, $J$ = 8.0 Hz, 3H, OCH$_2$C$H_3$). $^{13}$C NMR, HSQC, HMBC (101 MHz, $Tcl_2$, 100 °C) $\delta$ [ppm] = 156.8 (C-4′), 156.4 ('*C*═O), 155.5 (C-3⁗), 154.0 (C-3″), 151.1 (C-5″), 149.9 (C-4‴), 149.9 (C-6), 148.4 (C-2⁗), 144.6 (C-7), 139.0 (C-4″), 134.2 (C-1″), 132.2 (C-1′), 130.6 (C-2′, C-6′), 130.4 (C-4a), 130.0 (C-8a), 129.7 (C-1‴), 121.5 (C-6‴), 118.9 (C-8), 118.1 (C-2‴), 117.1 (C-3′, C-5′), 114.8 (C-5‴), 114.1 (C-5), 111.6 (C-6″), 108.7 (C-2″), 105.0 (C-1⁗), 61.2 (OC$H_2$–CH$_3$), 60.9 (4″-OC$H_3$), 60.7 ('OC$H_2$–CH$_3$), 56.8 (2⁗-OC$H_3$), 56.7 (4″-OC$H_3$ or 3″-OC$H_3$), 56.7 (4″-OC$H_3$ or 3″-OC$H_3$), 56.6 (6-OC$H_3$), 55.8 (C-1), 42.2 (NC$H_2$–CH$_2$, C-α), 38.6 (C-3), 36.2 (NCH$_2$–C$H_2$), 28.4 (C-4), 14.6 (OCH$_2$C$H_3$, 'OCH$_2$C$H_3$). The resonance of *C*═O could not be identified. IR (ATR): $\tilde{\nu}$ [cm$^{-1}$] = 2930, 2851, 1692, 1584, 1505, 1424, 1229, 1085, 1028, 941, 830, 767. HRMS (ESI): $m/z$ calcd for $[C_{43}H_{50}N_2O_{11} + K]^+$ 809.3052, found: 809.3045.

### (±)-Tetrandrine (*rac*-1) and (±)-isotetrandrine (*rac*-2)

To a suspension of $LiAlH_4$ (19 mg, 0.49 mmol) in anhydrous THF (3 mL), a solution of carbamate **15** (45.0 mg, 0.0609 mmol of either (1*R*,1′*S*)/(1*S*,1′*R*) or (1*R*,1′*R*)/(1*S*,1′*S*) diastereomer) in anhydrous THF (2 mL) was added dropwise under nitrogen atmosphere. The mixture was refluxed for 6 h. After cooling to 0 °C deionized water (5 mL) was added very slowly. The mixture was brought to pH 12–14 with sodium hydroxide solution (2 M) and extracted with ethyl acetate (4 × 20 mL). The combined organic phases were dried over anhydrous $Na_2SO_4$ and concentrated *in vacuo* to afford a yellow oil. Purification was accomplished by flash column chromatography (dichloromethane → 1% triethylamine and 2% methanol in dichloromethane, $R_f$ = 0.18). Racemic tetrandrine (*rac*-**1**) was obtained from (1*R*,1′*R*)/(1*S*,1′*S*)-**15** as colourless needles (37.0 mg, 0.0594 mmol, 98%) and racemic isotetrandrine (*rac*-**2**) from (1*R*,1′*S*)/(1*S*,1′*R*)-**15** as pale yellow prisms (37.3 mg, 0.0599 mmol, 98%), both after recrystallization from acetone. For the separation of the mixtures of diastereomers resulting from intramolecular *N*-acyl Pictet–Spengler reactions of **22** and **23** a preparative TLC method described by Lu *et al.*[47] was used with some modifications (0.5% triethylamine and 7.5% methanol in chloroform, $R_f$ (*rac*-**1**) = 0.32; $R_f$ (*rac*-**2**) = 0.22). Alternatively, preparative HPLC was performed on a Macherey-Nagel Nucleodur® 100–5 column (5 μm, 250 × 10 mm), eluent 1% methanol and 0.1% diethylamine in chloroform; flow rate 7.0 mL min$^{-1}$; temperature 25 °C; UV-detection at $\lambda$ = 283 nm; ($R_t$ (*rac*-**1**) = 4.11 min; $R_t$ (*rac*-**2**) = 4.93 min).

(±)-Tetrandrine (*rac*-**1**): Purity (HPLC) = 98% ($\lambda$ = 210 nm). Mp: 217–220 °C (literature: 252–253 °C (racemic tetrandrine)[62]). $^1$H NMR, COSY (500 MHz, $CDCl_3$) $\delta$ [ppm] = 7.34 (dd, $J$ = 8.2, 2.2 Hz, 1H, H-14′ or H-10′), 7.14 (dd, $J$ = 8.2, 2.5 Hz, 1H, H-13′ or H-11′), 6.88 (dd, $J$ = 8.2, 1.6 Hz, 1H, H-14), 6.86 (d, $J$ = 8.1 Hz, 1H, H-13), 6.80 (dd, $J$ = 8.2, 2.6 Hz, 1H, H-13′ or H-11′), 6.55 (d, $J$ = 1.7 Hz, 1H, H-10), 6.51 (s, 1H, H-5′), 6.30 (s, 1H, H-5), 6.30 (dd, $J$ = 8.3, 2.2 Hz, 1H, H-14′ or H-10′), 5.99 (s, 1H, H-8′), 3.93 (s, 3H, 12-OC$H_3$), 3.87 (dd, $J$ = 11.0, 5.6 Hz, 1H, H-1′), 3.75 (s, 3H, 6-OC$H_3$), 3.73 (s, 1H, H-1), 3.55–3.48

(m, 1H, H-3), 3.43 (ddd, $J$ = 12.6, 10.0, 5.9 Hz, 1H, H-3′), 3.37 (s, 3H, 6′-OC$H_3$), 3.25 (dd, $J$ = 12.5, 5.7 Hz, 1H, H-α′), 3.19 (s, 3H, 7-OC$H_3$), 2.99–2.89 (m, 3H, H-3, H-4, H-4′), 2.89–2.84 (m, 1H, H-3′), 2.80 (t, $J$ = 11.7 Hz, 1H, H-α′), 2.75–2.72 (m, 1H, H-4′), 2.70 (dd, $J$ = 14.2, 10.2 Hz, 1H, H-α), 2.62 (s, 3H, 2′-NC$H_3$), 2.52 (d, $J$ = 13.7 Hz, 1H, H-α), 2.45–2.39 (m, 1H, H-4), 2.33 (s, 3H, 2-NC$H_3$). $^{13}$C NMR, HSQC, HMBC (151 MHz, $CDCl_3$) $\delta$ [ppm] = 153.9 (C-12′), 151.5 (C-6), 149.5 (C-11), 148.7 (C-6′), 148.6 (C-8), 147.2 (C-12), 143.9 (C-7′), 138.0 (C-7), 135.4 (C-9′), 135.1 (C-9), 132.8 (C-14′ or C-10′), 130.3 (C-14′ or C-10′), 128.3 (C-4a), 128.2 (C-8a′), 128.1 (C-4a′), 123.1 (C-8a), 122.9 (C-14), 122.1 (C-13′ or 11′), 122.0 (C-13′ or 11′), 120.3 (C-8′), 116.4 (C-10), 112.9 (C-5′), 111.7 (C-13), 105.9 (C-5), 64.1 (C-1′), 61.6 (C-1), 60.4 (7-OC$H_3$), 56.3 (12-OC$H_3$), 56.0 (6′-OC$H_3$), 56.0 (6-OC$H_3$), 45.4 (C-3′), 44.3 (C-3), 42.8 (2′-NC$H_3$), 42.5 (2-NC$H_3$), 42.1 (C-α), 38.4 (C-α′), 25.4 (C-4′), 22.2 (C-4). The NMR data are identical with those of an authentic sample of tetrandrine. IR (ATR): $\tilde{\nu}$ [cm$^{-1}$] = 2940, 2838, 1579, 1506, 1446, 1410, 1355, 1268, 1213, 1121, 1023, 844, 767, 744. HRMS (ESI): $m/z$ calcd for $[C_{38}H_{42}N_2O_6 + H]^+$ 623.3116, found: 623.3111.

(±)-Isotetrandrine (*rac*-**2**): Purity (HPLC) = 97% ($\lambda$ = 210 nm). Mp: 175.5–182.0 °C (literature: 166–168 °C (enantiopure isotetrandrine[28]) A melting point of racemic isotetrandrine is not published yet). $^1$H NMR, COSY (500 MHz, $CDCl_3$) $\delta$ [ppm] = 7.27 (dd, $J$ = 8.4, 2.3 Hz, 1H, H-14′ or H-10′), 7.10 (dd, $J$ = 8.2, 2.5 Hz, 1H, H-13′ or H-11′), 6.83–6.77 (m, 2H, H-13, H-14), 6.67–6.63 (m, 1H, H-13′ or H-11′), 6.53 (s, 1H, H-5′), 6.48–6.37 (m, 2H, H-10, H-14′ or H-10′), 6.27 (s, 1H, H-5), 5.98 (s, 1H, H-8′), 3.92 (s, 3H, 12-OC$H_3$), 3.88–3.81 (m, 2H, H-1, H-1′), 3.75 (s, 3H, 6-OC$H_3$), 3.61 (s, 3H, 6′-OC$H_3$), 3.44–3.36 (m, 1H, H-3′), 3.33–3.21 (m, 2H, H-3, H-α′), 3.13 (s, 3H, 7-OC$H_3$), 3.03 (d, $J$ = 14.2 Hz, 1H, H-α), 2.96–2.86 (m, 3H, H-4, H-4′, H-α′), 2.85–2.76 (m, 3H, H-3, H-4′, H-3′), 2.60 (d, $J$ = 10.4 Hz, 1H, H-α), 2.57 (s, 3H, 2′-NC$H_3$), 2.45–2.31 (m, 1H, H-4), 2.26 (s, 3H, 2-NC$H_3$). $^{13}$C NMR, HSQC, HMBC (151 MHz, $CDCl_3$) $\delta$ [ppm] = 154.2 (12′), 152.0 (C-6), 150.0 (C-6′), 149.7 (C-11), 148.5 (C-4a), 147.1 (C-12), 143.8 (C-7′), 137.3 (C-7), 135.4 (C-9′), 132.2 (C-14′ or C-10′), 130.3 (C-14′ or 10′), 129.0 (C-4a′), 127.9 (C-8a′), 122.9 (C-14), 122.2 (C-13′ or C-11′), 121.8 (C-13′ or C-11′), 120.7 (C-8a), 120.0 (C-8′), 116.0 (C-9), 111.5 (C-13), 111.4 (C-5′), 105.7 (C-5), 64.0 (C-1′), 62.1 (C-1), 60.6 (7-OC$H_3$), 56.2 (12-OC$H_3$), 55.9 (6-OC$H_3$), 55.7 (6′-OC$H_3$), 46.3 (C-3′), 43.0 (2′-NC$H_3$), 42.8 (2-NC$H_3$), 38.9 (C-α), 37.9 (C-α′), 25.9 (C-4′), 23.2 (C-4). The resonances of C-3 and C-8 could not be identified. IR (ATR): $\tilde{\nu}$ [cm$^{-1}$] = 2933, 2834, 1582, 1506, 1445, 1413, 1260, 1229, 1114, 1030, 973, 865, 837, 772. HRMS (ESI): $m/z$ calcd for $[C_{38}H_{42}N_2O_6 + H]^+$ 623.3116, found: 623.3108. The NMR data are in accordance with published data.[63]

## Computational details

**Structure preparation.** All four macrocyclic intermediate structures as shown in Fig. 3 as well as a single molecule of dichloromethane (DCM) were built and minimized in Avogadro.[64]

**Parameterization.** The General Amber Force Field[61] parameters were used for all molecules. Charges for each intermediate structure were derived as follows: the antechamber module of AmberTools17 was used for calculating initial atomic charges on the AM1 level applying the bond charge correction and a net atomic charge of 1. Using Amber16,[60] 20.000 steps of initial conjugate-gradient minimization were performed for all structures, which were subsequently heated up to 300 K and simulated in gas phase for 4 μs. The trajectory was clustered according to the dihedral torsions of the macrocycle using cpptraj.[65] The representative structures of the first 10 clusters were optimized with the Gaussian09[66] program package on the HF/6-31G(d) level of theory and charges were fit to the electrostatic potential calculated according to the Merz–Singh–Kollman scheme.[67] Those 10 conformations were used as input structures for a multi-configurational RESP procedure to derive the final point charges. For the solvent the minimized DCM conformation was used for a charge derivation applying single-configurational RESP.

**Conformational sampling.** All Molecular Dynamics (MD) simulations in this study were carried out with Amber16.[60] Each intermediate structure, prepared as described in the previous paragraph, was placed inside a truncated octahedron, which was solvated with DCM molecules within a 20 Å region around the solute and a chloride ion for neutralization. A series of minimizations was performed to achieve a target density of 1.0 g cm$^{-3}$. Each system was heated to a target temperature of 258.15 K (−15 °C) to mimic the most favorable experimental conditions (see entry 3 in Table 3). The heating was performed over 150 ps with positional constraints on all atoms with a force constant of 3.0 kcal mol$^{-1}$ Å$^{-1}$ while heating to 20 K. Afterwards the constraints were removed from non-solute atoms while heating to 200 K. In the final step the unconstraint system was further heated up to 258.15 K. All heatup steps were performed in the NVT ensemble, whereas for all following simulations NPT ensemble was used. For pressure regulation the Berendsen barostat[68] and for temperature regulation the Langevin thermostat[69] with a collision frequency of 4.0 ps$^{-1}$ were used. Throughout the simulation, bonds involving hydrogen atoms were constrained using the SHAKE[70] algorithm, electrostatic energies were calculated using the Particle Mesh Ewald method[71] and periodic boundary conditions were applied. All simulations were performed with a time step of 1 fs and a 12 Å cutoff for non-bonded interactions, employing the *pmemd.cuda* engine of Amber16[60] on graphics processing units with mixed precision mode.[60]

For each intermediate two replica simulations were performed and the simulations were continued until 150 conformations could be extracted from the combined replica trajectories, which featured a distance smaller than 3.1 Å (3.2 Å) between atoms C-1′ and C-8a′ (C-1 and C-8a), *i.e.* the two atoms forming the final bond. It has to be mentioned that in the first 1000 ns less than 100 suitable structures were sampled for intermediates of route 2b, which is why the simulation was increased to 2000 ns. This way, the same amount of structures (150) could be extracted for intermediates of route 2a and 2b. These sets of structures represent possible starting conformations for the final reaction and were thus named "pre-reac-

tion ensemble" and analyzed further regarding their orientation around the second stereo center. This analysis revealed a structural preference of the C1-*S* intermediate of route 2a favouring tetrandrine formation compared to the enantiomeric counterpart (C1-*R* intermediate) that lacks a conformational preference (see results section). Thus, to rule out possible sampling issues, four additional replica trajectories for both intermediates of route 2a were simulated for additional 1000 ns each and a larger set of pre-reaction conformers could be extracted from all combined trajectories, see next paragraph.

**Dihedral analysis.** For all structures of the pre-reaction ensembles the relative pre-reaction orientation (pre-*S* or pre-*R*) at the second stereocenter was analyzed manually based on the relative position of the hydrogen atom. Table S1‡ lists the amount of structures within the first 150 pre-reaction conformations sampled for route 2a and 2b, respectively, that originate from either intermediate of each route and are oriented towards either pre-*S* or pre-*R* at the second stereocenter. With 4 additional replicas sampled for route 2a the pre-reaction ensembles increased to a total amount of 547 conformations, for which the same analysis was repeated corresponding to the numbers in brackets in Table S1.‡ Furthermore, for the pre-reaction ensemble the position of ring A′ (A) relative to the second stereocenter was determined visually and defined in a binary fashion as + (corresponding to the methoxy group(s) flipped backward in Fig. 4) and – (corresponding to the methoxy group(s) flipped forward in Fig. 4).

**Potential energies.** The average potential energies for the intermediate structures of routes 2a were calculated with our in-house program DynaDock[72] by averaging over all pre-reaction conformers.

## Conflicts of interest

There are no conflicts to declare.

## Acknowledgements

Financial support was provided for F. B. by the Deutsche Forschungsgemeinschaft (project BR1034/7-1) and for M. M. and I. A. by the Deutsche Forschungsgemeinschaft (SFB749/C08 and SFB1035/A10, CIPSM).

## References

1 N. Bhagya and K. R. Chandrashekar, *Phytochemistry*, 2016, **125**, 5–13.
2 N. Bhagya and K. R. Chandrashekar, *Biomed. Pharmacother.*, 2018, **97**, 624–632.
3 H. Kondo and K. Yano, *Yakugaku Zasshi*, 1928, **48**, 107–123.
4 K. K. Chen and A. L. Chen, *J. Biol. Chem.*, 1935, **109**, 681–685.
5 C.-Y. Kwan and F. Achike, *Acta Pharmacol. Sin.*, 2016, **23**, 1057–1068.
6 V. F. King, M. L. Garcia, D. Himmel, J. P. Reuben, Y. K. Lam, J. X. Pan, G. Q. Han and G. J. Kaczorowski, *J. Biol. Chem.*, 1988, **263**, 2238–2244.
7 S. Patel, *Sci. Signaling*, 2015, **8**, re7.
8 Y. Sakurai, A. A. Kolokoltsov, C.-C. Chen, M. W. Tidwell, W. E. Bauta, N. Klugbauer, C. Grimm, C. Wahl-Schott, M. Biel and R. A. Davey, *Science*, 2015, **347**, 995–998.
9 O. N. P. Nguyen, C. Grimm, L. S. Schneider, Y.-K. Chao, C. Atzberger, K. Bartel, A. Watermann, M. Ulrich, D. Mayr, C. Wahl-Schott, M. Biel and A. M. Vollmar, *Cancer Res.*, 2017, **77**, 1427–1438.
10 D. Falzarano and H. Feldmann, *Science*, 2015, **347**, 947–948.
11 M. Shamma, *The isoquinoline alkaloids: chemistry and pharmacology*, Academic Press, New York, 1972, ch. 5, vol. 25.
12 D. Longley and P. Johnston, *J. Pathol.*, 2005, **205**, 275–292.
13 P. Joshi, R. A. Vishwakarma and S. B. Bharate, *Eur. J. Med. Chem.*, 2017, **138**, 273–292.
14 S. Dewanjee, T. Dua, N. Bhattacharjee, A. Das, M. Gangopadhyay, R. Khanra, S. Joardar, M. Riaz, V. Feo and M. Zia-Ul-Haq, *Molecules*, 2017, **22**, 871.
15 R. J. Kelly, R. W. Robey, C. C. Chen, D. Draper, V. Luchenko, D. Barnett, R. K. Oldham, Z. Caluag, A. R. Frye, S. M. Steinberg, T. Fojo and S. E. Bates, *Oncologist*, 2012, **17**, 512–e523.
16 C.-Z. Wu, L. Lai, X. Hu, R.-R. Lei and Y.-F. Yang, *J. Asian Nat. Prod. Res.*, 2013, **15**, 993–1002.
17 Q.-H. Yang, C.-S. Jiang, T. Jin, J.-F. Xu, T.-L. Qu, Y.-W. Guo and Z.-B. Zhao, *J. Asian Nat. Prod. Res.*, 2018, 1–11, DOI: 10.1080/10286020.2018.1478817.
18 Z. Cao, M. Wright, J. Cheng, X. Huang, L. Liu, L. Wu and P. Yang, *Oncol. Rep.*, 2014, **32**, 1211–1217.
19 J. Lan, N. Wang, L. Huang, Y. Liu, X. Ma, H. Lou, C. Chen, Y. Feng and W. Pan, *Eur. J. Med. Chem.*, 2017, **127**, 554–566.
20 J. Lan, L. Huang, H. Lou, C. Chen, T. Liu, S. Hu, Y. Yao, J. Song, J. Luo, Y. Liu, B. Xia, L. Xia, X. Zeng, Y. Ben-David and W. Pan, *Eur. J. Med. Chem.*, 2018, **143**, 1968–1980.
21 J. Song, J. Lan, C. Chen, S. Hu, J. Song, W. Liu, X. Zeng, H. Lou, Y. Ben-David and W. Pan, *MedChemComm*, 2018, **9**, 1131–1141.
22 V. Calvillo-Páez, R. R. Sotelo-Mundo, M. Leyva-Peralta, J. C. Gálvez-Ruiz, D. Corona-Martínez, R. Moreno-Corral, R. Escobar-Picos, H. Höpfl, O. Juárez-Sánchez and K. O. Lara, *Chem.-Biol. Interact.*, 2018, **286**, 34–44.
23 Y. Tian and J. Zheng, in *Advances in Molecular Toxicology*, ed. J. C. Fishbein and J. M. Heilman, Academic Press, Cambridge, San Diego, Oxford, London, 2017, ch. 6, vol. 11, pp. 241–272.
24 H. Jin, L. Li, D. Zhong, J. Liu, X. Chen and J. Zheng, *Chem. Res. Toxicol.*, 2011, **24**, 2142–2152.
25 Y. Tian, S. Shen, Y. Jiang, Q. Shen, S. Zeng and J. Zheng, *Arch. Toxicol.*, 2016, **90**, 1737–1748.
26 L. Tainlin, H. Tingyi, Z. Changqi, Y. Peipei and Z. Qiong, *Ecotoxicol. Environ. Saf.*, 1982, **6**, 528–534.
27 Y. Inubushi, Y. Masaki, S. Matsumoto and F. Takami, *Tetrahedron Lett.*, 1968, **9**, 3399–3402.

 

28 Y. Inubushi, Y. Masaki, S. Matsumoto and F. Takami, *J. Chem. Soc. C*, 1969, 1547–1556.
29 J. Qingping, Y. Bin, G. Zhenzhen, D. Yanqun, C. Yu, J. Yan, Z. Mingqiang and Y. Weicheng, *CN*109942593, 2019.
30 D. L. Comins, P. M. Thakker, M. F. Baevsky and M. M. Badawi, *Tetrahedron*, 1997, **53**, 16327–16340.
31 J. F. Hartwig, *Angew. Chem., Int. Ed.*, 1998, **37**, 2046–2067.
32 D. M. T. Chan, K. L. Monaco, R.-P. Wang and M. P. Winters, *Tetrahedron Lett.*, 1998, **39**, 2933–2936.
33 J. J. Maresh, A. A. Ralko, T. E. Speltz, J. L. Burke, C. M. Murphy, Z. Gaskell, J. K. Girel, E. Terranova, C. Richtscheidt and M. Krzeszowiec, *Synlett*, 2014, 2891–2894.
34 S. G. Davies, E. C. Goddard, P. M. Roberts, A. J. Russell, A. D. Smith, J. E. Thomson and J. M. Withey, *Tetrahedron: Asymmetry*, 2016, **27**, 274–284.
35 A. Yokoyama, T. Ohwada and K. Shudo, *J. Org. Chem.*, 1999, **64**, 611–617.
36 C. H. Burgos, T. E. Barder, X. Huang and S. L. Buchwald, *Angew. Chem., Int. Ed.*, 2006, **45**, 4321–4326.
37 D. Ma and Q. Cai, *Org. Lett.*, 2003, **5**, 3799–3802.
38 J. Wang and G. Evano, *Org. Lett.*, 2016, **18**, 3542–3545.
39 J. Shi, J. Wu, C. Cui and W.-M. Dai, *J. Org. Chem.*, 2016, **81**, 10392–10403.
40 L. Shen, C. J. Simmons and D. Sun, *Tetrahedron Lett.*, 2012, **53**, 4173–4178.
41 D. Maiti and S. L. Buchwald, *J. Org. Chem.*, 2010, **75**, 1791–1794.
42 L. Navarro and M. D. Pujol, *Tetrahedron Lett.*, 2015, **56**, 1812–1815.
43 S. Kang, R. J. Ono and C. W. Bielawski, *J. Polym. Sci., Part A: Polym. Chem.*, 2013, **51**, 3810–3817.
44 S. J. Gharpure, A. M. Sathiyanarayanan and P. Jonnalagadda, *Tetrahedron Lett.*, 2008, **49**, 2974–2978.
45 C. G. Caldwell, Y.-C. Chiang, C. Dorn, P. Finke, J. Hale, M. Maccoss, S. Mills and A. Robichaud, *WO*98/17660, 1998.
46 J. Kayhan, M. J. Wanner, S. Ingemann, J. H. van Maarseveen and H. Hiemstra, *Eur. J. Org. Chem.*, 2016, 3705–3708.
47 S.-T. Lu, I.-L. Tsai and S.-P. Leou, *Phytochemistry*, 1989, **28**, 615–620.
48 E. Mons, M. J. Wanner, S. Ingemann, J. H. van Maarseveen and H. Hiemstra, *J. Org. Chem.*, 2014, **79**, 7380–7390.
49 D. L. Comins and M. M. Badawi, *Tetrahedron Lett.*, 1991, **32**, 2995–2996.
50 C. Gremmen, M. J. Wanner and G.-J. Koomen, *Tetrahedron Lett.*, 2001, **42**, 8885–8888.
51 M. Chrzanowska, A. Grajewska and M. D. Rozwadowska, *Chem. Rev.*, 2016, **116**, 12369–12465.
52 R. E. Gawley, G. Hart, M. Goicoechea-Pappas and A. L. Smith, *J. Org. Chem.*, 1986, **51**, 3076–3078.
53 N. Uematsu, A. Fujii, S. Hashiguchi, T. Ikariya and R. Noyori, *J. Am. Chem. Soc.*, 1996, **118**, 4916–4917.
54 B. Horst, M. J. Wanner, S. I. Jørgensen, H. Hiemstra and J. H. van Maarseveen, *J. Org. Chem.*, 2018, **83**, 15110–15117.
55 L. Evanno, J. Ormala and P. M. Pihko, *Eur. J. Chem.*, 2009, **15**, 12963–12967.
56 N. Blank and T. Opatz, *J. Org. Chem.*, 2011, **76**, 9777–9784.
57 I. Ugur, M. Schroft, A. Marion, M. Glaser and I. Antes, *J. Mol. Model.*, 2019, **25**, 197.
58 S. Wang, A. H. Crevenna, I. Ugur, A. Marion, I. Antes, U. Kazmaier, M. Hoyer, D. C. Lamb, F. Gegenfurtner, Z. Kliesmete, C. Ziegenhain, W. Enard, A. Vollmar and S. Zahler, *Sci. Rep.*, 2019, **9**, 9731.
59 B. Eyermann, M. Meixner, H. Brötz-Oesterhelt, I. Antes and S. A. Sieber, *ChemBioChem*, 2020, **21**, 235–240.
60 D. A. Case, R. M. Betz, D. S. Cerutti, T. E. Cheatham, III, T. A. Darden, R. E. Duke, T. J. Giese, H. Gohlke, A. W. Goetz, N. Homeyer, S. Izadi, P. Janowski, J. Kaus, A. Kovalenko, T. S. Lee, S. LeGrand, P. Li, C. Lin, T. Luchko, R. Luo, B. Madej, D. Mermelstein, K. M. Merz, G. Monard, H. Nguyen, H. T. Nguyen, I. Omelyan, A. Onufriev, D. R. Roe, A. Roitberg, C. Sagui, C. L. Simmerling, W. M. Botello-Smith, J. Swails, R. C. Walker, J. Wang, R. M. Wolf, X. Wu, L. Xiao and P. A. Kollman, *AMBER 2016*, University of California, San Francisco, 2016.
61 J. Wang, R. M. Wolf, J. W. Caldwell, P. A. Kollman and D. A. Case, *J. Comput. Chem.*, 2004, **25**, 1157–1174.
62 S. M. Kupchan, N. Yokoyama and B. S. Thyagarajan, *J. Pharm. Sci.*, 1961, **50**, 164–167.
63 H. Guinaudeau, A. J. Freyer and M. Shamma, *Nat. Prod. Rep.*, 1986, **3**, 477–488.
64 M. D. Hanwell, D. E. Curtis, D. C. Lonie, T. Vandermeersch, E. Zurek and G. R. Hutchison, *J. Cheminf.*, 2012, **4**, 17.
65 D. R. Roe and T. E. Cheatham, *J. Chem. Theory Comput.*, 2013, **9**, 3084–3095.
66 M. J. Frisch, G. W. Trucks, H. B. Schlegel, G. E. Scuseria, M. A. Robb, J. R. Cheeseman, G. Scalmani, V. Barone, B. Mennucci, G. A. Petersson, H. Nakatsuji, M. Caricato, X. Li, H. P. Hratchian, A. F. Izmaylov, J. Bloino, G. Zheng, J. L. Sonnenberg, M. Hada, M. Ehara, K. Toyota, R. Fukuda, J. Hasegawa, M. Ishida, T. Nakajima, Y. Honda, O. Kitao, H. Nakai, T. Vreven, J. A. Montgomery, Jr., J. E. Peralta, F. Ogliaro, M. Bearpark, J. J. Heyd, E. Brothers, K. N. Kudin, V. N. Staroverov, R. Kobayashi, J. Normand, K. Raghavachari, A. Rendell, J. C. Burant, S. S. Iyengar, J. Tomasi, M. Cossi, N. Rega, J. M. Millam, M. Klene, J. E. Knox, J. B. Cross, V. Bakken, C. Adamo, J. Jaramillo, R. Gomperts, R. E. Stratmann, O. Yazyev, A. J. Austin, R. Cammi, C. Pomelli, J. W. Ochterski, R. L. Martin, K. Morokuma, V. G. Zakrzewski, G. A. Voth, P. Salvador, J. J. Dannenberg, S. Dapprich, A. D. Daniels, Ö. Farkas, J. B. Foresman, J. V. Ortiz, J. Cioslowski, and D. J. Fox, *Gaussian 09, Revision E.01*, Gaussian, Inc., Wallingford, CT, 2009.
67 U. C. Singh and P. A. Kollman, *J. Comput. Chem.*, 1984, **5**, 129–145.
68 H. J. C. Berendsen, J. P. M. Postma, W. F. v. Gunsteren, A. DiNola and J. R. Haak, *J. Chem. Phys.*, 1984, **81**, 3684–3690.

69 W. F. van Gunsteren and H. J. C. Berendsen, *Angew. Chem., Int. Ed. Engl.*, 1990, **29**, 992–1023.
70 J.-P. Ryckaert, G. Ciccotti and H. J. C. Berendsen, *J. Comput. Phys.*, 1977, **23**, 327–341.
71 T. Darden, D. York and L. Pedersen, *J. Chem. Phys.*, 1993, **98**, 10089–10092.
72 I. Antes, *Proteins: Struct., Funct., Bioinf.*, 2010, **78**, 1084–1104.